Shapes and gravitational fields of rotating two-layer Maclaurin ellipsoids: Application to planets and satellites

Gerald Schubert [1], John D. Anderson[2], Keke Zhang[3], Dali Kong[3], and Ravit Helled[1]

[1]Department of Earth and Space Sciences

University of California, Los Angeles, CA 900951567, USA

[2]Jet Propulsion Laboratory [*],

4800 Oak Grove Drive, Pasadena, CA 91109

[3] Department of Mathematical Sciences

College of Engineering, Mathematics and Physical Sciences

University of Exeter, Exeter, UK

Abstract

The exact solution for the shape and gravitational field of a rotating two-layer Maclaurin ellipsoid of revolution is compared with predictions of the theory of figures up to third order in the small rotational parameter of the theory of figures. An explicit formula is derived for the external gravitational coefficient J_2 of the exact solution. A new approach to the evaluation of the theory of figures based on numerical integration of ordinary differential equations is presented. The classical Radau-Darwin formula is found not to be valid for the rotational parameter $\epsilon_2 = \Omega^2/(2\pi G\rho_2) \geq 0.17$ since the formula then predicts a surface eccentricity that is smaller than the eccentricity of the core-envelope boundary. Interface eccentricity must be smaller than surface eccentricity. In the formula for ϵ_2, Ω is the angular velocity of the two-layer body, ρ_2 is the density of the outer layer, and G is the gravitational constant. For an envelope density of 3000 kg m^{-3} the failure of the Radau-Darwin formula corresponds to a rotation period of about 3 hr. Application of the exact solution and the theory of figures is made to models of Earth, Mars, Uranus, and Neptune. The two-layer model with constant densities in the layers can provide realistic approximations to terrestrial planets and icy outer planet satellites. The two-layer model needs to be generalized to allow for a continuous envelope (outer layer) radial density profile in order to realistically model a gas or ice giant planet.

[*]Retiree

1 Introduction

Kong et al. (2010) have presented an exact theory for the rotational distortion of a rotating two-layer spherical body with a constant density core surrounded by an envelope (outer layer) with a different constant density. The solution for the case when the core and envelope have equal densities, the Maclaurin ellipsoids, was obtained more than 250 years ago and attracted the attention of such notables as d'Alembert, Clairaut, Euler, Laplace, Legendre, Poisson and Gauss. The solutions are discussed in Chandrasekhar (1969, Ellipsoidal Figures of Equilibrium) and Lamb (1932, Hydrodynamics). Until the work of Kong et al. (2010), the classical solution for the constant density Maclaurin ellipsoid had not been generalized to a body with non-uniform density. Instead, approximate solutions, for bodies with density increasing from the surface to the center, have been developed by geophysicists interested in the internal structures of the Earth and planets. The approximate solutions fall under the umbrella of the theory of figures (Zharkov and Trubitsyn, 1978, Physics of Planetary Interiors) and rely on the smallness of a rotational parameter that measures the distortion of a rotating body. In this paper we refer to the theory developed by Zharkov and Trubitsyn (1978) for the shapes of fluid bodies as the theory of figures. The rotational distortions of the Earth and planets are indeed small, but it is important to accurately determine the small distortions to correctly infer the interior structures of the bodies. Accordingly, the theory of figures has been developed to high order in the small rotational parameter.

While the two-layer spherical body with constant core and envelope densities is too simple a model for the careful study of most planets, the exact solution for the rotational distortion of such a body provides a benchmark against which the accuracy and range of validity of approximate solutions and numerical models can be evaluated. In this paper we compare results from the exact solution for the rotating two-layer Maclaurin ellipsoids to those obtained using the Radau-Darwin approximation and other simplifications based on the theory of figures. We derive formulae for the rotationally distorted two-layer sphere using the theory of figures valid to third order in the small rotational parameter and assess these results against the exact solution. Application of the exact theory is made to the Earth and planets while keeping in mind the limitations of using a two-layer model to represent these bodies. Both the theory of figures and the exact theory of Kong et al. (2010) assume hydrostatic equilibrium of the rotating body.

2 Exact Solution for a Rotating Two-Layer Spherical Body

We consider the distortion of a two-layer spherical body rotating with constant angular velocity Ω. The core has radius r_1 and constant density ρ_1. The core is surrounded by a spherical shell envelope of outer radius r_2 and constant density ρ_2. The exact solution for the distortion is presented in Kong et al. (2010). Here, we summarize only a few things necessary for making use of the theory. The problem is completely specified

by three dimensionless parameters, the core-envelope density ratio ρ_1/ρ_2, the fractional volume of the core $Q_{\rm V} = (r_1/r_2)^3$, and the rotation parameter

$$\epsilon_2 = \frac{\Omega^2}{(2\pi {\rm G}\rho_2)}, \tag{1}$$

where G is the gravitational constant. Among the quantities derivable from the solution are the eccentricities of the total (gravity) equipotential surfaces, and, in particular, the eccentricities of the core-envelope interface and the surface, E_1 and E_2 , respectively. The total or gravity potential is the sum of the gravitational potential and the rotational potential. Surfaces of constant total (gravity) potential are shown in Figure 1 for the cases (a) $Q_{\rm V} = 0.5$, $\rho_1/\rho_2 = 2$, $\epsilon_2 = 0.18$ and (b) $Q_{\rm V} = 0.25$, $\rho_1/\rho_2 = 2$, $\epsilon_2 = 0.05$. The eccentricity of these total potential isosurfaces is plotted as a function of radius in Figure 2. The eccentricity of total potential isosurfaces generally decreases inward except for the region of the interface where eccentricity changes rapidly and non-monotonically. Eccentricity has a local maximum at the interface and a local minimum in the envelope just above the interface. Eccentricity decreases monotonically with decreasing radius inside the core; the decrease is very gradual until the center of the core is approached.

The coefficient J_2 of the external gravitational field is an important quantity to determine because it can be measured by a spacecraft flying by or orbiting a planet. For the rotating two-layer body, J_2 can be found from the exact solution by proceeding as follows. In a spherical coordinate system, the axisymmetric gravitational potential $V_{\rm g}$ outside a uniformly rotating body can be expanded as

$$V_{\rm g}(r,\theta) = -\frac{{\rm G}M}{r}\left[1 - J_2\left(\frac{R_{\rm e}}{r}\right)^2 P_2(\cos\theta) + \cdots\right], \tag{2}$$

where M is the mass of the body, P_{2n} are the Legendre polynomials, $R_{\rm e}$ is the equatorial radius of the body, r is the radial distance from the center of the body ($r > R_{\rm e}$), and θ is the colatitude of the observation point with respect to the rotation axis. On the spherical surface $r = R_{\rm e}$, the expansion becomes

$$V_{\rm g}(r = R_{\rm e},\theta) = -\frac{{\rm G}M}{R_{\rm e}}\left[1 - J_2 P_2(\cos\theta) + \cdots\right]. \tag{3}$$

By determining $V_{\rm g}(r = R_{\rm e},\theta)$ from the exact solution, J_2 can be calculated from the projection of the potential onto the expansion (3).

The gravitational potential expansion in the spheroidal coordinate system employed in the exact solution is

$$\begin{aligned} V_{\rm g}(\xi,\eta) = {} & -2\pi {\rm G}c_2^2 \sum_{l=0}^{\infty} i(2l+1)P_l(\eta) \\ \times {} & \left[Q_l(i\xi)\int_0^{\xi}\int_{-1}^{1}[(\xi')^2 + (\eta')^2]P_l(\eta')P_l(i\xi')\rho'{\rm d}\eta'{\rm d}\xi' \right. \\ + {} & \left. P_l(i\xi)\int_{\xi}^{\xi_{\rm o}}\int_{-1}^{1}[(\xi')^2 + (\eta')^2]P_l(\eta')Q_l(i\xi')\rho'{\rm d}\eta'{\rm d}\xi'\right] \end{aligned} \tag{4}$$

(Kong et al., 2010). In (4), ξ, η are spheroidal coordinates with focal length c_2, P_l and Q_l are Legendre functions of the first and second kind, respectively, and i is the square root of -1. In addition ρ' is the density as a function of ξ', η', and $\xi_{\rm o}$ is the value of ξ at the outer free surface. Evidently, we need to make the transformation from spheroidal coordinates to spherical coordinates before computing $V_{\rm g}(r,\theta)$ from (4). The relationship between the spherical and spheroidal coordinates is (Kong et al., 2010).

$$r\cos\theta \;=\; c_2\sqrt{(1+\xi^2)(1-\eta^2)}, \tag{5}$$

$$r\sin\theta \;=\; c_2\xi\eta \tag{6}$$

Taking $r = R_{\rm e}$ and using the fact that $c_2 = R_{\rm e}E_2$, we find the transformation in the form

$$\cos\theta \;=\; E_2\sqrt{(1+\xi^2)(1-\eta^2)}, \tag{7}$$

$$\sin\theta \;=\; E_2\xi\eta \tag{8}$$

Equations (7) and (8) enable us to derive ξ and η as functions of θ

$$\eta^2 \;=\; \frac{\sqrt{(1-E_2^2)^2+4E_2^2\cos^2\theta}-(1-E_2^2)}{2E_2^2} \tag{9}$$

$$\xi^2 \;=\; \eta^2+\frac{1}{E_2^2}-1 \tag{10}$$

With (9) and (10), we are able to derive the gravitational potential as a function of the spherical coordinate θ.

When $V_{\rm g}(r=R_{\rm e},\theta)$ is available, we project it onto the spherical harmonic expansion to obtain J_2. We expect the expansion in the form

$$V_{\rm g}\left(r=R_{\rm e},\theta\right)=\sum_l\sqrt{\frac{2l+1}{2}}C_lP_l(\cos\theta), \tag{11}$$

where

$$C_l=\sqrt{\frac{2l+1}{2}}\int_0^\pi V_{\rm g}\left(r=R_{\rm e},\theta\right)P_l(\cos\theta)\sin\theta{\rm d}\theta. \tag{12}$$

By comparing (11) and (3), we find

$$\frac{1}{2}C_0 \;=\; -\frac{{\rm G}M}{R_{\rm e}} \tag{13}$$

$$\frac{5}{2}C_2 \;=\; \frac{{\rm G}M}{R_{\rm e}}J_2, \tag{14}$$

from which J_2 can be simply calculated as

$$J_2=\frac{-5C_2}{C_0}. \tag{15}$$

3 Comparison with the Radau-Darwin Approximation

The Radau-Darwin approximate formula can be used to predict the flattening or eccentricity of the outer surface of a rotating body (Radau, 1885; Darwin, 1900). The formula relates the normalized axial moment of inertia C/Ma_2^2 (C is the axial moment of inertia around the rotation axis, M is the total mass of the body, and a_2 is the equatorial radius) to the second degree Love number h_2

$$\frac{C}{Ma_2^2} = \frac{2}{3}\left[1 - \frac{2}{5}\frac{(5-h_2)^{1/2}}{h_2^{1/2}}\right] \tag{16}$$

(Zharkov and Trubitsyn, 1978). The Love number gives the flattening of the surface $f_2 = (a_2 - c_2)/a_2$ by

$$f_2 = \frac{qh_2}{2} \tag{17}$$

(Zharkov and Trubitsyn, 1978), where q is the small rotational parameter

$$q = \frac{\Omega^2 a_2^3}{\mathrm{G}M} \tag{18}$$

The flattening and eccentricity of the surface of the body are related by

$$f_2 = 1 - \left(1 - E_2^2\right)^{1/2} \tag{19}$$

Equations (16)-19) are often used in planetary physics to determine the moment of inertia of a body whose shape (flattening), rotation rate, mass, and equatorial radius are known. With f_2 and q known, (17) gives h_2 and (16) gives C/Ma_2^2. Alternative to the flattening, the gravitational coefficient J_2 can be used to infer the axial moment of inertia since to a first approximation J_2 and f_2 are related by

$$f_2 = \frac{3}{2}J_2 + \frac{1}{2}m \tag{20}$$

(Zharkov and Trubitsyn, 1978), where m is the small rotational parameter given by

$$m = \frac{\Omega^2 s_2^3}{\mathrm{G}M} \tag{21}$$

and s_2 is the mean radius of the body (the radius of a spherical body with the same volume as the rotationally-distorted body). The Radau-Darwin formula can be rewritten in terms of J_2 and m by using (17) and (21) to eliminate h_2.

The Radau-Darwin formula can be used to predict the flattening or eccentricity of the surface of the rotating two-layer spherical body and the result compared with the value of the eccentricity from the exact solution of Kong et al. (2010). The normalized moment of inertia of a two-layer sphere is

$$\frac{C}{Mr_2^2} = \frac{2}{5}\left[\frac{\rho_1}{\overline{\rho}} + \frac{(\rho_1 - \rho_2)}{\overline{\rho}}\left(\frac{r_1}{r_2}\right)^5\right] \tag{22}$$

This can be rewritten in terms of the dimensionless variables that characterize the solution of Kong et al. (2010) as

$$\frac{C}{Mr_2^2} = \frac{2}{5}\left[\left(1+Q_{\rm V}^{5/3}\right)\left\{Q_{\rm V}+\frac{(1-Q_{\rm V})}{\rho_1/\rho_2}\right\}^{-1} - Q_{\rm V}^{5/3}\left\{1-Q_{\rm V}+\left(\frac{\rho_1}{\rho_2}\right)Q_{\rm V}\right\}^{-1}\right] \tag{23}$$

Given $Q_{\rm V}$ and ρ_1/ρ_2, the dimensionless moment of inertia is calculated from (23), and h_2 follows from (16). The flattening and eccentricity of the model surface is then obtained from (17) and (19).

Table 1 compares the exact solution for the eccentricities of the interface E_1 and surface E_2 (evaluated using the theory of Kong et al. (2010)) with the eccentricity of the surface from the Radau-Darwin formula E_2^{R-D} for the case $Q_{\rm V} = 0.5$ and $\rho_1/\rho_2 = 2$ for different values of the rotation parameter ϵ_2. The agreement between the approximate and exact solutions is quite good in this case for all the rotation rates considered. Strictly speaking, the Radau-Darwin approximation can be said to be invalid for values of $\epsilon_2 > 0.17$ since the Radau-Darwin formula predicts surface eccentricities less than the interface eccentricities, when in fact, the interface eccentricity should be less than the surface eccentricity. That this is the case can be qualitatively understood by considering the flattening of a rotating sphere of uniform density ρ. The flattening is proportional to ρ^{-1}. In a body that has density increasing with depth, the flattening or eccentricity of equipotential surfaces should accordingly decrease with depth.

4 Comparison with the Theory of Figures for the Generalized Roche Model

The generalized Roche model is a special case of the two-layer model of this paper in which the envelope density $\rho_2 = 0$. An analytic formula for the flattening of total potential isosurfaces, correct to second order in the rotational parameter m, is given in Zharkov and Trubitsyn (1978). (We also derive this formula later in Section 5.8.1, which discusses the generalized Roche model from our perspective on the theory of figures.) The flattening of the surface according to this formula $f_2^{\rm ToF}$ is given by

$$f_2^{\rm ToF} = \frac{1}{2}m\left(1+\frac{3}{2}\beta_C^5\right) + \frac{1}{8}m^2\left(\beta_C^5 + \frac{20}{7}\beta_C^8 - \frac{33}{28}\beta_C^{10}\right) \tag{24}$$

where $\beta_C = r_1/r_2 = Q_{\rm V}^{1/3}$. The rotation parameter m is defined in (21)for $s_2 = r_2$. It is related to the parameters of the exact theory by

$$m = \frac{3\left(\epsilon_2\rho_2\right)}{2Q_{\rm V}\rho_1} \tag{25}$$

where $\epsilon_2\rho_2$ is independent of ρ_2 (see (1)). The flattening of the interface according to the second order theory of figures ToF is

$$f_1^{\rm ToF} = \frac{5}{4}m\beta_c^3 + \frac{75}{224}m^2\beta_c^6 \tag{26}$$

Equation (26) follows from (58) and (87) and (91) with $\beta = \beta_c$ in the expressions for F_1 and F_2.

Table 2 compares the eccentricity of the surface and the interface of several models computed using the exact theory with values obtained from (24) and (26) for the generalized Roche model with the help of (19) to convert to the eccentricity $E_2^{\rm ToF}$. For the exact theory we consider the sequence of values of ρ_2/ρ_1 equal to 10^{-2}, 10^{-3}, and 10^{-4} to compare with the Roche model result that takes $\rho_2 = 0$. For the cases considered in the table the theory of figures to second order in m only slightly underestimates the surface and interface eccentricities.

A formula for the surface flattening correct to third order in m is given by combining $f\,(\beta_c)$ from (26) with F_{31} given by (92).

5 First-Order Theory of Figures for Synchronous Rotation and Tides

The theory of figures dates back to Clairaut, who in 1743 derived an integrodifferential equation for the flattening of a rotating body in hydrostatic equilibrium (HE), but with a non-uniform density distribution in the interior (Kaula, 1968). Clairaut's theory represents a first order perturbation theory to a non-rotating spherical configuration with arbitrary density distribution in layers, the level surfaces, or the surfaces of constant total potential, the sum of the gravitational potential and the non-inertial centrifugal potential (zero in the spherical configuration). The small rotational parameter m for the perturbation theory is related to the body's rotation period P, its mean radius R, and its total mass M by

$$m = \left(\frac{2\pi}{P}\right)^2 \left(\frac{R^3}{\mathrm{G}M}\right) \quad \text{(compare (21))} \tag{27}$$

where G is the gravitational constant given by $(6.674215 \pm 0.000092) \times 10^{-11}$ m^3 kg^{-1} s^{-2} (Gundlach and Merkowitz, 2000). Often, the combination GM is known from orbital dynamics to greater accuracy than G itself, and the total mass is a derived parameter given by GM/G, accurate to essentially the same fractional error as G, or 14 parts per million. The mean radius R (also denoted by s_2 in (21)) is the radius of a uniform sphere equal in density to the planet's mean density ρ_0 or,

$$\rho_0 = \frac{3\,(\mathrm{G}M)}{4\pi \mathrm{G} R^3} \tag{28}$$

The flattening f is defined in terms of the equatorial radius a and polar radius c by,

$$f = \frac{a-c}{a} \tag{29}$$

In the first order Clairaut theory, the rotating mass configuration consists of continuous layers of concentric ellipsoids of revolution, each with its own density and flattening. The configuration is defined in terms of a single variable, the normalized mean radius $\beta = s/R$, which labels the level surfaces. The actual mean

radius s, in metric units, can always be recovered by multiplying β by the given mean radius R of the planet. The density $\rho(\beta)$ of a particular level surface can also be normalized to the given mean density, so that $\delta(\beta) = \rho(\beta)/\rho_0$.

For perturbations of higher order than the first, these definitions can all be retained. However, the level surfaces are no longer ellipsoids of revolution. Even so, the radius r of a particular level surface can be expressed in terms of the mean radius s by a distortion to the usual polar coordinate equation for an ellipse. For the third order theory, the radius r can be expressed as a function of the polar angle θ (colatitude), the flattening f, and two higher-order, spheroidal shape parameters k and h, as follows (Zharkov and Trubitsyn, 1978).

$$r(\theta) = a\left[1 - f\cos^2\theta - \left(\frac{3}{8}f^2 + k\right)\sin^2 2\theta + \frac{1}{4}\left(\frac{1}{2}f^3 + h\right)\left(1 - 5\sin^2\theta\right)\sin^2 2\theta\right] \tag{30}$$

It is convenient to express the radius in terms of μ, the cosine of θ. Then the mean radius is given by the integral

$$s^3 = \frac{1}{2}\int_{-1}^{1} r^3(\mu)\,\mathrm{d}\mu \tag{31}$$

and the expression for the radius becomes

$$r = R\beta\sum_{i=0}^{\infty} a_{2i}\mu^{2i} \tag{32}$$

Consistent with (30) and (31), the coefficients to third order are

$$\begin{aligned}
a_0 &= \left(1 + \frac{1}{3}f + \frac{2}{9}f^2 + \frac{14}{81}f^3 + \frac{8}{15}k + \frac{26}{105}h + \frac{16}{63}fk\right) \\
a_2 &= -\left(f + \frac{11}{6}f^2 + \frac{49}{18}f^3 + 4k + 4h + \frac{28}{15}fk\right) \\
a_4 &= \frac{3}{2}\left(f^2 + \frac{10}{3}f^3 + \frac{8}{3}k + 6h + \frac{8}{9}fk\right) \\
a_6 &= -\frac{5}{2}\left(f^3 + 2h\right)
\end{aligned} \tag{33}$$

This is an alternating series that converges absolutely, and the error in the partial sum is less than the absolute value of the next term in the series.

Equation (32) is fundamental to the theory of figures. With it, a coordinate transformation between Cartesian coordinates (x,y,z) and generalized coordinates (β, ϕ, μ) can be defined by

$$\begin{aligned}
x &= r\cos\phi\sqrt{1-\mu^2} \\
y &= r\sin\phi\sqrt{1-\mu^2} \\
z &= r\mu
\end{aligned} \tag{34}$$

Because of axial symmetry, the azimuthal coordinate ϕ can be integrated out of the problem immediately. The series coefficients a_{2i} are functions of β only, by means of the shape functions f,k,h. The differential volume element $\mathrm{d}\tau$ can be found from the Jacobian determinant of the transformation.

For example, after integrating for the coordinates ϕ and μ, the gravitational coefficients J_n in the external gravitational potential are given by Zharkov and Trubitsyn (1978),

$$J_n = -\int \delta(\beta)\,\beta^n P_n(\mu)\;\mathrm{d}\tau = -\int_0^1 \delta(\beta)\;\mathrm{d}\left[\beta^{n+3}\phi_n(\beta)\right], \tag{35}$$

where P_n is the Legendre polynomial of degree n. The functions ϕ_n are derived in A to third order by means of a definite integral in μ from minus one to plus one. The only integral that remains in (35) for further evaluation is the integral in β, which depends on the given density distribution $\delta(\beta)$.

Similarly, the principal moments of inertia, C along the polar axis, and A along an equatorial axis, can be expressed as third-order series. All quantities are thereby normalized to the total mass M and powers of the mean radius R, so that the external gravitational potential function V is expressed as

$$V = \frac{\mathrm{G}M}{r}\left[1 - \sum_{i=1}^{\infty}\left(\frac{R}{r}\right)^{2i} J_{2i} P_{2i}(\mu)\right] \tag{36}$$

The measured gravitational coefficients J_{2i} can be determined from orbital dynamics, as is $\mathrm{G}M$. They are most often referred to a reference value for the equatorial radius a_{ref}. However, they can be referred to R by multiplying each observed value of degree $2i$ by $(a_{\mathrm{ref}}/R)^{2i}$, consistent with the computed values from (35).

The usefulness of the theory of figures is that a reasonable density distribution $\delta(\beta)$ can be found that minimizes the weighted sum of squares WSOS for the measured coefficients, the method of weighted least squares. The minimization function in terms of the observed coefficients $\hat{J}_{2i}$, along with their standard errors σ_{2i}, and the computed values J_{2i} from (35) is

$$WSOS = \sum_{i=1}^{\infty}\left(\frac{\hat{J}_{2i} - J_{2i}}{\sigma_{2i}}\right)^2 \tag{37}$$

If the orbital dynamics is limited, such that there are strong correlations among the coefficients, the minimization can be generalized to include the covariance matrix Γ for the $\hat{J}_{2i}$ from the analysis of the orbital data. The residuals $\hat{J}_{2i} - J_{2i}$ are placed in a column matrix z and WSOS is defined by the matrix operation $z^T\Gamma^{-1}z$, with z^T the transpose of z.

In principle the theory can be extended to arbitrary order in the small rotational parameter m. However, it becomes quite cumbersome for orders greater than three. Nevertheless, all expressions required for a fifth-order theory have been published by Zharkov and Trubitsyn (1976). In the fifth-order theory the radius r is still normalized to the mean radius s, but (32) is replaced by the following Legendre series, valid to arbitrary order n

$$\frac{r}{s} = 1 + \sum_{j=2}^{n} s_{0j} m^j + \sum_{j=1}^{n} m^j s_{2j} P_{2j}(\mu) \tag{38}$$

This expression can be substituted into (31) and expanded in a power series in m to order n. Then coefficients of m^i for powers of i greater than or equal to 2 can be set to zero. This yields $n-1$ equations in the $n-1$

coefficients s_{0j}, which can all be evaluated. For example, at fifth order the values are

$$\begin{aligned} s_{02} &= -\frac{1}{5}s_2^2 \\ s_{03} &= -\frac{2}{105}s_2^3 \\ s_{04} &= -\frac{1}{315}\left(35s_4^2 + 18s_2^2 s_4\right) \\ s_{05} &= -\frac{2}{17325}\left(33s_2^5 + 250 s_2 s_4^2\right) \end{aligned} \tag{39}$$

A substitution of the s_{0j} values so determined into (38) yields the n^{th} order expression for r/s, comparable to (32), the third-order expression in the spheroidal functions f, k, and h. The parameter s_2 in (38) and (39) is not the mean radius parameter used in (21).

The easiest way to compare the theory with observation is to refer the measured gravitational harmonics to the mean radius of the planet. The advantage is that (35) directly represents what is being measured. However, the mean radius of a planet depends on its rotation period, which is not always known, and which may not even be constant throughout the interior. In this sense, the measured equatorial radius is a more fundamental observational constraint. Therefore, when the measured J_n are referred to the equatorial radius, the theoretical values given by (35) must be multiplied by the ratio $(s/a)^n$. This ratio can be found from the inverse of the expression for r/s, with μ set equal to zero. With this approach, care is required in order to make sure that higher order terms in $(s/a)^n$ do not enter into the theoretical expression for J_n and bias it. Furthermore, this is true in general. If one is computing a first-order Clairaut spheroid, it is important to make sure the series are always strictly truncated at first order. The same can be said for a second-order Darwin spheroid, or to any spheroid of arbitrary order n.

5.1 The Level Surfaces

The application of (35) requires that the functions $s_{2j}(\beta)$, or alternatively $f(\beta)$, $h(\beta)$, and $k(\beta)$ in the expression for r/s of (32), be found for a given interior density distribution, expressed in terms of the normalized density $\delta(\beta)$. This is accomplished by finding the level surfaces on which the interior gravitational potential is a constant. The interior potential at a normalized mean radius β is determined by the amount of mass interior to the level surface, an integral over the volume from zero to β, plus the amount of mass exterior to the level surface, an integral from β to one. Let the gravitational moments of the mass lying internal to β be given by $S_{2j}(\beta)$. The normalized potential V_0 from the mass interior to β is given by the expansion of s/r in Legendre polynomials. We illustrate this procedure for the spheroidal functions to order three. The more general procedure for the s_{2j} functions to arbitrary order is similar.

The first step is to invert the expression for r/s in (32) and expand it in a series to order three in the small rotational parameter m. The result is a function in even powers of μ. Next, the Legendre polynomials

in μ can be inverted to any arbitrary degree to obtain powers of μ in terms of the polynomials. For third order in m the result is

$$\begin{aligned}
\mu^2 &= \frac{1}{3}\left[1 + 2P_2\left(\mu\right)\right] \\
\mu^4 &= \frac{1}{35}\left[7 + 20P_2\left(\mu\right) + 8P_4\left(\mu\right)\right] \\
\mu^6 &= \frac{1}{231}\left[33 + 110P_2\left(\mu\right) + 72P_4\left(\mu\right) + 16P_6\left(\mu\right)\right]
\end{aligned} \tag{40}$$

The next step in the procedure is to substitute the powers of μ given by (40) into the series for s/r. The result is an expansion of s/r in a series of Legendre polynomials in the form

$$V_0 = \frac{s}{r} = \sum_{j=0}^{n} C_{2j}^0 P_{2j}\left(\mu\right) \tag{41}$$

For the spheroidal functions, the coefficients C_{2j}^0 can be written as

$$\begin{aligned}
C_0^0 &= 1 + \frac{8}{45}f^2 + \frac{584}{2835}f^3 + \frac{64}{315}fk \\
C_2^0 &= \frac{2}{3}f + \frac{31}{63}f^2 + \frac{76}{189}f^3 - \frac{2}{21}h + \frac{8}{21}k + \frac{88}{315}fk \\
C_4^0 &= -\frac{4}{35}f^2 - \frac{172}{1155}f^3 - \frac{192}{385}h - \frac{32}{35}k - \frac{416}{1155}fk \\
C_6^0 &= \frac{8}{231}f^3 + \frac{80}{231}h - \frac{128}{231}fk
\end{aligned} \tag{42}$$

This completes the expansion for the zero-degree gravitational moment S_0, which is basically a mass function given by

$$S_0 = \frac{3}{\beta^3}\int_0^{\beta} z^2\delta\left(z\right)\,\mathrm{d}z \tag{43}$$

For any interior density distribution given by $\delta(\beta)$, the function S_0 must be equal to one at the surface of the planet, where β is equal to one. Otherwise the interior model will not be consistent with the observed mass and mean radius.

In general, the gravitational moments S_{2i} are included in the level-surface theory by series expansion in powers of the inverted r/s in (41) times the appropriate higher-degree Legendre polynomial, as follows

$$V_i = \left(\frac{s}{r}\right)^{2i+1} P_{2i}\left(\mu\right) \qquad i = 0, 1, 2, \cdots, n \tag{44}$$

The series expansion to order m for a particular degree $2i$ is carried out to order $n - i$. The powers of μ given by (40) are substituted into the series for V_i. The result is an expansion in Legendre polynomials that can be written

$$V_i = \sum_{j=0}^{n} C_{2j}^i P_{2j}\left(\mu\right) \qquad i = 0, 1, 2, \cdots, n \tag{45}$$

The evaluation of the coefficients C_{2j}^i for the spheroidal functions is given in A for orders 1, 2 and 3. The coefficients for order zero are given by (42).

The gravitational moments S'_{2i} for the potential exterior to the level surface labeled by β require potential functions V'_i, which are defined by

$$V'_i = \left(\frac{r}{s}\right)^{2i} P_{2i}(\mu) \qquad i = 0, 1, 2, \cdots, n \tag{46}$$

After similar expansion in powers of m as for V_i, the potentials for mass between β and the surface at $\beta = 1$ can be expressed in terms of coefficients $C^{ii'}_{2j}$ by

$$V'_i = \sum_{j=0}^{n} C^{ii'}_{2j} P_{2j}(\mu) \qquad i = 0, 1, 2, \cdots, n \tag{47}$$

The coefficients $C^{ii'}_{2j}$ are given to third order in A.

So far we have been concerned with the expansion of the internal gravitational potential to order n in a series of Legendre polynomials of degree $2n$ in the general coordinate μ. However, the planet is in rotation about its principal axis of maximum moment of inertia, the z axis. In this rotating non-inertial coordinate system the planet deviates from a sphere because of a centrifugal force generated by a rotation in inertial space, a rotation with respect to the "fixed stars". Relativistic corrections to this Newtonian model are ignored in the theory of figures for planets. Therefore the centrifugal force per unit mass can be represented by the following potential function V_{rot}

$$V_{\text{rot}} = \frac{1}{2}\left(\frac{2\pi}{P}\right)^2 r^2 \sin^2\theta \tag{48}$$

This potential function can be made consistent with the gravitational potentials V_i and V'_i by replacing the period P by the smallness parameter m according to (27), by replacing μ by the Legendre polynomial P_2 according to (40), and by normalizing to the gravitational potential GM/R at the surface. The result is (Zharkov and Trubitsyn, 1978)

$$Q = \frac{1}{3} m \left(\frac{r}{s}\right)^2 [1 - P_2(\mu)] \tag{49}$$

The centrifugal potential Q can be expanded to arbitrary order by means of (38) or to third order by (32). The third order coefficients corresponding to the third order coefficients for V_i and V'_i are

$$\begin{aligned}
Q_0 &= m\left(\frac{1}{3} + \frac{4}{45}f + \frac{2}{189}f^2 + \frac{16}{315}k\right) \\
Q_2 &= -m\left(\frac{1}{3} + \frac{20}{63}f + \frac{38}{189}f^2 + \frac{16}{45}k\right) \\
Q_4 &= m\left(\frac{8}{35}f + \frac{76}{231}f^2 + \frac{32}{55}k\right) \\
Q_6 &= -m\left(\frac{32}{231}f^2 + \frac{64}{231}k\right)
\end{aligned} \tag{50}$$

The small rotational parameter m enters explicitly in the theory of figures by means of the centrifugal potential Q.

All the coefficients derived so far can be collected into complete expressions for the internal potentials A_i on the level surface labeled by β. These potentials to arbitrary order can be written as

$$A_i = \sum_{j=0}^{n} \left(C_{2j}^{i} S_{2j} + C_{2j}^{i\prime} S_{2j}^{\prime} \right) + Q_i \qquad i = 0, 2, 4, \cdots, 2n \tag{51}$$

The gravitational moments can be written in terms of the following integrals (Zharkov and Trubitsyn, 1978)

$$\begin{aligned} S_i &= \frac{1}{\beta^{i+3}} \int_0^{\beta} \delta(z) \, \mathrm{d}\left[z^{i+3} \phi_i \right] \\ S_i^{\prime} &= \beta^{i-2} \int_{\beta}^{1} \delta(z) \, \mathrm{d}\left[z^{2-i} \phi_i^{\prime} \right] \end{aligned} \tag{52}$$

The functions ϕ_i and $\phi_i^{\prime}$ represent the integral of the gravitational moments over μ as follows

$$\begin{aligned} \phi_i &= \frac{3}{2(i+3)} \int_{-1}^{1} P_i(\mu) \left(\frac{r}{s} \right)^{i+3} \mathrm{d}\mu \qquad i = 0, 2, 4, \cdots, 2n \\ \phi_i^{\prime} &= \frac{3}{2(2-i)} \int_{-1}^{1} P_i(\mu) \left(\frac{r}{s} \right)^{2-i} \mathrm{d}\mu \qquad i = 0, 2, 4, \cdots, 2n \end{aligned} \tag{53}$$

When i is equal to 2, the integration for $\phi_2^{\prime}$ must be carried out as a special limiting case. The integral is

$$\phi_2^{\prime} = \frac{3}{2} \int_{-1}^{1} P_2(\mu) \ln\left(\frac{r}{s} \right) \mathrm{d}\mu \tag{54}$$

The functions under the integrals for ϕ_i and $\phi_i^{\prime}$ can be expanded to arbitrary order in m and integrated. The results to order three are given in A. Results to order 5 by means of (38) are given by Zharkov and Trubitsyn (1976).

Evaluations of A_0, A_2, A_4 and A_6 are given in Appendix B. In order that the potential be a constant on level surfaces, all potentials of order greater than zero must be zero. This means that any A_i with i equal to 2 or greater can be multiplied through by a constant. It also means that A_2 can be used to solve for m, as it appears explicitly in Q_2. By substituting this value of m into the higher-degree potentials, A_4, A_6 and higher, they can be simplified. They do not contain m explicitly. A_0 is the only potential function that is not zero. For this reason it represents the total internal potential at normalized mean radius β, with the centrifugal term included in the potential. It is the potential that enters in the equation of HE. The pressure $p(\beta)$ on a level surface and the total gravitational potential $U(\beta)$ can be normalized by the following relations involving the given mass M and mean radius R for the planet

$$\begin{aligned} \chi(\beta) &= \frac{Rp(\beta)}{\mathrm{G}M\rho_0} \\ A_0(\beta) &= \frac{RU(\beta)}{\mathrm{G}M} \end{aligned} \tag{55}$$

In terms of these normalized variables, the equation of HE in the interior is given by Zharkov and Trubitsyn (1978)

$$\frac{\mathrm{d}\chi}{\mathrm{d}\beta} = \delta \frac{\mathrm{d}\left(\beta^2 A_0 \right)}{\mathrm{d}\beta} \tag{56}$$

5.2 Solution to the Level-Surface Problem

The objective of a solution to the level-surface problem is to find the gravitational moments and the shape of the planet at its surface, and to compare the theoretical result with what is observed for the surface shape and external gravitational field. This result depends on the interior normalized density distribution $\delta(\beta)$, which can be a given function, as in the two-zone model treated here, or it can be obtained from a known equation of state (EOS) by including (56) in the solution of the overall problem. When the EOS is given for the internal material as a function $\chi(\delta)$, most likely in zones, the following differential equation for δ can be included in the solution for the theoretical interior model

$$\left(\frac{\mathrm{d}\chi}{\mathrm{d}\delta}\right)\frac{\mathrm{d}\delta}{\mathrm{d}\beta} = \delta\frac{\mathrm{d}\left(\beta^2 A_0\right)}{\mathrm{d}\beta} \tag{57}$$

This suggests that it might be useful to have the level-surface problem not in the form of integrodifferential equations, but in the form of differential equations only. An advantage of this approach is that a numerical solution to a set of differential equations (ODE) can be carried out to high precision, in fact to far more precision than needed to justify the accuracy of the observational constraints on a static model. An alternative method used in a previous paper (Anderson and Schubert, 2007) can cause precision problems. The method expresses the shape coefficients f, k and h, or s_{2i}, as polynomials in β, and forces the polynomial coefficients to satisfy the equations $A_{2i} = 0$. The problem with this approach is that a finite number of polynomial coefficients can never be found that satisfy the equations everywhere on the interval $0 \le \beta \le 1$. Numerical compromises must be made in order to satisfy the equations on average over the interval. With the ODE approach, the solution for the shape parameters can be automated.

Using this ODE approach, we first express the shape coefficients as power series in the small rotational parameter m. We illustrate the method for f, k and h, and use it for the two-zone model, but it can be extended to higher orders as well. The three spheroidal functions can be written as

$$\begin{aligned} f(\beta) &= mF_1(\beta) + m^2F_2(\beta) + m^3F_3(\beta) \\ k(\beta) &= m^2K_2(\beta) + m^3K_3(\beta) \\ h(\beta) &= m^3H_3(\beta) \end{aligned} \tag{58}$$

The first step in the procedure is to substitute these expressions for f, k and h into the functions ϕ_{2i} and ϕ'_{2i} given in Appendix C and to drop terms of order higher than three. The next step is to substitute the resulting power series into the expressions for S_{2i} and S'_{2i} given by (52). Finally substitute the resulting gravitational moments and the shape functions f, k and h into the expressions for A_2, A_4 and A_6 given in Appendix B. Then expand to order three in m. This completes the setup of the level-surface problem for the ODE approach.

The lowest-order level-surface potential is A_2 to the first order in m. Call it A_{21}. It is obtained as the

coefficient of m for A_2 from the setup of the problem. It can be written as

$$A_{21} = -\frac{1}{2} + S_0 F_1(\beta) - \frac{3}{5}\int_\beta^1 \delta(z) F_1'(z)\, \mathrm{d}z - \frac{3}{5\beta^5}\int_0^\beta z^4 \delta(z)\left(5F_1(z) + zF_1'(z)\right) \mathrm{d}z = 0 \tag{59}$$

where S_0 can be evaluated by the integral of (43). Differentiate A_{21} once with respect to β to obtain

$$A_{21}' = \frac{3}{\beta^6}\int_0^\beta z^4 \delta(z)\left[5F_1(z) + zF_1'(z)\right] \mathrm{d}z - \frac{1}{\beta} S_0\left[3F_1(\beta) - \beta F_1'(\beta)\right] = 0 \tag{60}$$

Multiply this derivative by β^6 and differentiate once again. The result is

$$\left(\beta^6 A_{21}'\right)' = 6\beta^4 \delta(\beta)\left[F_1(\beta) + \beta F_1'(\beta)\right] - \beta^4 S_0\left[6F_1(\beta) - \beta^2 F_1''(\beta)\right] = 0 \tag{61}$$

This last equation (61) is Clairaut's differential equation for the flattening function. However, the first two equations contain integrals that are not known, and they will enter into higher-order ODE. Therefore, we solve for the two integrals from the two equations (59) and (60) and at the same time solve for the second derivative of F_1 from the third equation (61). This establishes a procedure for all higher orders. The result is

$$\begin{aligned}
&\int_0^\beta z^4\ \delta(z)\left[5F_1(z) + zF_1'(z)\right] \mathrm{d}z = \beta^5 S_0 F_1(\beta) - \frac{1}{3}\beta^6 S_0 F_1'(\beta) \\
&\int_\beta^1 \delta\ \ (z) F_1'(z)\, \mathrm{d}z = -\frac{5}{6} + \frac{2}{3} S_0 F_1(\beta) + \frac{1}{3}\beta S_0 F_1'(\beta) \\
&F_1''\ \ (\beta) = \frac{6}{\beta^2} F_1(\beta) - \frac{6}{\beta^2}\left(\frac{\delta(\beta)}{S_0}\right) F_1(\beta) - \frac{6}{\beta}\left(\frac{\delta(\beta)}{S_0}\right) F_1'(\beta)
\end{aligned} \tag{62}$$

The ODE in (62) can be solved for F_1 and F_1' and the result can be substituted into the two integrals. The solution to the ODE to first order in m and the corresponding two integrals are now available for higher order ODE. The boundary conditions on the solution are discussed in section 5.3 and they are applied to the two-zone model in section 5.6. Note that the density function that completely determines F_1 is given by the ratio δ/S_0.

The next function for consideration is K_2. It is derived from the coefficient A_{42} of m^2 in A_4. This time A_{42} is divided by β^2 and differentiated. Then the result of that first differentiation is multiplied by β^{10} and differentiated once more. This establishes the procedure for all the shape functions. When A_6 is involved, it is divided by β^4 and differentiated. Then the result of that differentiation is multiplied by β^{14} and differentiated once more. The procedure can in principle be carried to higher orders. For each shape function, three equations are solved for two unknown integrals and the second derivative of that particular shape function. The sequence of steps for deriving the ODE is F_1, K_2, F_2, H_3, K_3, F_3, and so forth. The result can be expressed as a nonlinear homogeneous differential equation plus a function of β that is built

up by means of the sequence of derivations. We express the ODE in the form

$$\begin{aligned}
\beta^2 F_i'' + 6\beta\left(\frac{\delta}{S_0}\right)F_i' - 6\left(1-\frac{\delta}{S_0}\right)F_i &= G_{2i} \qquad i=1,2,3 \\
\beta^2 K_i'' + 6\beta\left(\frac{\delta}{S_0}\right)K_i' - 2\left(10-3\frac{\delta}{S_0}\right)K_i &= G_{4i} \qquad i=2,3 \\
\beta^2 H_i'' + 6\beta\left(\frac{\delta}{S_0}\right)H_i' - 6\left(7-\frac{\delta}{S_0}\right)H_i &= G_{6i} \qquad i=3
\end{aligned} \tag{63}$$

These equations differ in form because of the way k and h are defined in (30). The functions G_{ji} are given in Appendix D.

5.3 General Boundary Conditions

The derivatives of the shape functions at the surface where β is equal to one can be found sequentially, similar to the technique for finding the ODE. For the function F_1, the potential A_{21} is multiplied by β^5 and differentiated. This is done for A_{22} and A_{23} as well. For A_{42} and A_{43} the multiplier before differentiation is β^7, and for A_{63} it is β^9. The resulting derivatives are evaluated for β equal to one. Consequently, the integral with limits of integration from β to one is set to zero. The integral representing S_0 is evaluated at the surface such that S_0 is equal to one. The second derivatives are eliminated by substitution of the ODE, again evaluated at the surface. The resulting first derivatives of the potential functions multiplied by the appropriate β^i can be set to zero and all the derivatives of the shape functions at the surface boundary can be found sequentially. As a result, the surface boundary conditions are given by

$$\begin{aligned}
F_{11}' &= \frac{5}{2} - 2F_{11} \\
K_{21}' &= \frac{25}{16} - \frac{5}{4}F_{11} - 4K_{21} \\
F_{21}' &= -\frac{5}{12} + \frac{19}{42}F_{11} + \frac{1}{3}F_{11}^2 - 2F_{21} + \frac{8}{7}K_{21} \\
H_{31}' &= \frac{25}{8} + \frac{15}{4}F_{11} - 5F_{11}^2 - 6H_{31} - 2K_{21} \\
K_{31}' &= -\frac{25}{24} + \frac{25}{168}F_{11} + \frac{137}{168}F_{11}^2 - \frac{5}{4}F_{21} + \frac{12}{11}H_{31} + \frac{904}{231}K_{21} - \frac{524}{231}F_{11}K_{21} - 4K_{31} \\
F_{31}' &= \frac{155}{72} - \frac{143}{84}F_{11} - \frac{47}{147}F_{11}^2 + \frac{7}{9}F_{11}^3 + \frac{19}{42}F_{21} + \frac{2}{3}F_{11}F_{21} - 2F_{31} - \frac{92}{77}H_{31} \\
&\quad -\frac{68}{11}K_{21} + \frac{22}{2695}F_{11}K_{21} + \frac{8}{7}K_{31}
\end{aligned} \tag{64}$$

This gives the derivatives of the shape functions at the surface. One more set of boundary conditions is needed for a unique solution to the ODE, and hence for a unique interior model for a given density distribution $\delta(\beta)$, or for a unique EOS that can be integrated by (57) to yield a unique density distribution. One approach is to iterate on the surface functions, which must satisfy the boundary conditions given by (64), until finite functions are obtained at the origin. However, this iterative process can be tedious. An

alternative, which we adopt here, introduces a constant-density core into the interior density distribution. The core radius β_C can take on any value in the interval $0 < \beta_C \leq 1$, and in principle it can be arbitrarily small. However, as the core radius approaches zero, the numerical precision required to evaluate the shape functions at the core boundary becomes arbitrarily large. For every model, there is a practical lower limit to the core radius β_C. We illustrate this method of a core plus overlying envelope in Sec. 5.6.

5.4 Calculation of the Normalized Pressure in the Interior

To the first order in m, the pressure depends only on the density distribution. The differential equation for χ is simply (Zharkov and Trubitsyn, 1978)

$$\frac{\mathrm{d}\chi}{\mathrm{d}\beta} = \left[-S_0 + \frac{2}{3}m\right] \beta\delta\left(\beta\right) \tag{65}$$

The boundary condition for a solution to (65) is that χ is equal to zero at β equal to one. The density distribution can be piecewise continuous, as in the two-zone model considered here. However, the pressure and gravitational potential must be continuous over a density discontinuity. This implies that the spheroidal functions f, k and h (or the s_{2i} functions) and their first derivatives must be continuous throughout the interior. In addition, the derivative $\mathrm{d}\delta/\mathrm{d}\beta$ must be less than or equal to zero throughout the interior, so that the density either remains constant (incompressible material) or increases with depth. Also $\delta(\beta)$ must satisfy the boundary condition that the gravitational moment S_0 as given by (43) must be equal to one at the planet's surface. The surface is defined such that all the planetary mass is contained within the outermost level surface with β equal to one. Even so, the pressure and the density can be made to match a model atmosphere. The atmosphere is a part of the total mass. In that sense, it is more realistic to define the surface at the 100 mbar level in the atmosphere, near the top of the troposphere, not at a more standard one-bar level. Nevertheless, the one-bar level is an acceptable approximation to the surface. At least this approximation avoids the complication of treating the atmosphere as a separate zone in the level-surface computation. There is something to be said for separating the atmospheric modeling from the interior modeling, and simply making sure the two are consistent at the one-bar level. For one thing, the atmosphere is not static, but is dominated by observed zonal flows for all four giant planets in the solar system. The theory of figures is a static equilibrium theory. A level surface of one bar in the atmosphere is stretching the static assumption as it is. It is a reasonable level to stop the interior modeling. In order that both the density and the pressure go to zero at the surface, the density must go to zero at the surface. This introduces another constraint on the interior density distribution. A separate constraint is that the derivative of the density distribution at the surface is equal to the derivative in the atmosphere at the one bar level. With the inclusion of the constraint on S_0 previously mentioned, this results in a total of three constraints on the interior density distribution. Physically, these three constraints mean that the total mass of the model

is equal to the measured total mass of the planet, and that the interior density distribution matches the density distribution in the atmospheric model at the one-bar level.

By means of the derivation of the ODE for the shape functions in the interior, it is straightforward to derive the second and third order terms in the differential equation for the pressure. All the integrals necessary for an evaluation of A_0 are available from the derivation of the ODE. The first order term in (65) contains only zero-order shape functions. Similarly, the second order terms in the derivative of $\beta^2 A_0$ contains only first order terms in the shape functions. The right side of (56) can be expanded in powers of m, and each order can be integrated separately for purposes of obtaining the normalized pressure $\chi(\beta) = \chi_0(\beta) + m\chi_1(\beta) + m^2\chi_2(\beta) + m^3\chi_3(\beta)$ to third order. The four functions for the integrations are given by

$$\begin{aligned}
\frac{\mathrm{d}\left(\beta^2 A_{00}\right)}{\mathrm{d}\beta} &= -\beta S_0 \\
\frac{\mathrm{d}\left(\beta^2 A_{01}\right)}{\mathrm{d}\beta} &= \frac{2}{3}\beta \\
\frac{\mathrm{d}\left(\beta^2 A_{02}\right)}{\mathrm{d}\beta} &= \frac{8}{45}\beta\left(2F_1 + \beta F_1'\right) + \frac{4}{45}\beta S_0\left(5F_1^2 + 2\beta F_1 F_1' + \beta^2 F_1'^2\right) \\
\frac{\mathrm{d}\left(\beta^2 A_{03}\right)}{\mathrm{d}\beta} &= -\frac{8}{135}\beta\left[5F_1^2 - 6F_2 + 2\beta F_1 F_1' + \beta\left(\beta F_1'^2 - 3F_2'\right)\right] \\
&\quad + \frac{4}{2835}\beta S_0\left(385F_1^3 + 231\beta F_1^2 F_1'\right) \\
&\quad + \frac{24}{2835}\beta^2 S_0 F_1'\left[21F_2 + 12K_2 + \beta\left(2\beta F_1'^2 + 21F_2' + 12K_2'\right)\right] \\
&\quad + \frac{24}{2835}\beta S_0 F_1\left[105F_2 + 60K_2 + \beta\left(25\beta F_1'^2 + 21F_2' + 12K_2'\right)\right]
\end{aligned} \tag{66}$$

The pressure can be found by multiplying the four derivatives in (66) by the normalized density $\delta(\beta)$ and integrating, with the boundary condition $\chi(1)$ equal to zero.

The method described here can be applied to the simple case of a planet made up of incompressible material in HE. The normalized density is a constant equal to one, and the zero degree gravitational moment S_0 is also a constant equal to one. The ODE simplify considerably, but that fact can be ignored, and our general numerical procedure can be applied to the constant-density case. As a result, the numerical solution to the ODE yields the result

$$\begin{aligned}
f &= \frac{5}{4}m\left(1 + \frac{15}{56}m + \frac{925}{1568}m^2\right) \\
k &= 0 \\
h &= 0
\end{aligned} \tag{67}$$

The normalized axial moment of inertia C/Ma^2 for this configuration is equal to 2/5, independent of m. A numerical integration of the four pressure functions in (66), with $\delta(\beta)$ equal to one, yields the following

result for the normalized pressure

$$\chi = \left(1-\beta^2\right)\left(\frac{1}{2} - \frac{1}{3}m - \frac{41}{72}m^2 - \frac{1235}{2268}m^3\right) \tag{68}$$

In the above, the real numbers returned by the numerical integration have been replaced by nearby rational numbers with small denominator. This has only been done in (68).

The next simplest density distribution is the linear distribution. Because it implies compressible material, it is a far better approximation to a real planet than the constant-density model. The normalized density $\delta(\beta)$ is equal to $4(1-\beta)$. For purposes of applying our numerical procedure, we introduce a core of normalized radius β_C equal to 0.05. The normalized constant density in the core is equal to 3.85. The gravitational moment S_0 in the envelope is equal to $4-3\beta$. In this model, there is a negligible fractional core mass equal to 77/160000. The numerical integration is carried out in the envelope over the interval $0.05 \le \beta \le 1$.

5.5 Calculation of the Coefficients J_n in the Exterior Gravitational Potential

The solution to the differential equations to third order in the small rotational parameter m yields the six shape functions F_1, F_2, F_3, K_2, K_3, H_3. If good observations of the shape of the planet are available, such as for the Earth, these shape functions can be used directly to constrain the envelope density δ_E. However, for the outer planets, the measured zonal gravitational coefficients J_2, J_4 and J_6 provide far better constraints on δ_E. The calculated values of the three coefficients are given by (35).

The procedure for finding values of the gravitational coefficients in terms of the shape functions is to first express the coefficients as a truncated power series in m according to

$$\begin{aligned} J_2 &= mJ_{21} + m^2 J_{22} + m^3 J_{23} \\ J_4 &= m^2 J_{42} + m^3 J_{43} \\ J_6 &= m^3 J_{63} \end{aligned} \tag{69}$$

Next we recognize that the coefficients, when referenced to the equatorial radius a, are proportional to the gravitational moments S_n by

$$S_n = \left(\frac{a}{s}\right)^n J_n \tag{70}$$

and where, from (32) with μ set equal to zero

$$\frac{a}{s} = 1 + \frac{1}{3}f + \frac{2}{9}f^2 + \frac{14}{81}f^3 + \frac{26}{105}h + \frac{8}{15}k + \frac{16}{63}fk \tag{71}$$

Substitute (70) into the expressions for the potential functions A_2,A_4,A_6 given respectively by (107), (109), (110), and evaluate at the surface. Use the truncated series of (69) for the J_n and the similar series for the shape functions given in (58). The functions S_n' are all zero at the surface. Expand to order three in m. Since all the coefficients of powers of m are zero, this process yields six equations which can be solved for

the six J_n functions in terms of the six shape functions from the differential equations, again evaluated at the surface. The result is

$$
\begin{aligned}
J_{21} &= -\frac{1}{3} + \frac{2}{3}F_{11} \\
J_{22} &= \frac{2}{21}F_{11} - \frac{1}{3}F_{11}^2 + \frac{2}{3}F_{21} + \frac{8}{21}K_{21} \\
J_{23} &= -\frac{11}{147}F_{11}^2 + \frac{2}{21}F_{21} - \frac{2}{3}F_{11}F_{21} + \frac{2}{3}F_{31} - \frac{2}{21}H_{31} - \frac{16}{105}K_{21} + \frac{40}{147}F_{11}K_{21} + \frac{8}{21}K_{31} \\
J_{42} &= \frac{4}{7}F_{11} - \frac{4}{5}F_{11}^2 - \frac{32}{35}K_{21} \\
J_{43} &= -\frac{22}{49}F_{11}^2 + \frac{4}{5}F_{11}^3 + \frac{4}{7}F_{21} - \frac{8}{5}F_{11}F_{21} - \frac{192}{385}H_{31} + \frac{208}{385}K_{21} + \frac{3616}{2695}F_{11}K_{21} - \frac{32}{35}K_{31} \\
J_{63} &= -\frac{20}{21}F_{11}^2 + \frac{8}{7}F_{11}^3 + \frac{80}{231}H_{31} - \frac{160}{231}K_{21} + \frac{128}{77}F_{11}K_{21}
\end{aligned}
\tag{72}
$$

5.6 The Two-Layer Model

The two-layer model consists of a constant density core of normalized density δ_C, plus an envelope of normalized density δ_E. The envelope density can be a function of β, or even piecewise continuous in two or more zones overlying the constant-density core. The two densities are connected by means of the mass constraint implied by (43), and they must satisfy the following equation

$$\delta_C \beta_C^3 + 3\int_{\beta_C}^{1} \beta^2 \delta_E(\beta)\, \mathrm{d}\beta = 1 \tag{73}$$

A particular interior model is defined by the envelope density δ_E and the core radius β_C. The core density δ_C is a derived constant obtained from (73). As the core radius approaches zero, the core density approaches positive infinity. However, the core mass given by $\delta_C \beta_C^3$ is finite at the origin. For β_C arbitrarily small, the core mass can represent a point-mass core with mass greater than or equal to zero. Whatever the values for $\delta_E(\beta)$ and β_C, the ODE of (63) can be solved exactly in the core, and the second set of boundary conditions for the envelope integration can be found at the core-envelope boundary.

5.7 Solution to the Theory of Figures in a Constant-Density Core

The functions needed for the ODE of (63) are S_0 and δ/S_0. For a constant-density core, S_0 is simply δ_C and the ratio δ/S_0 is one. It follows from (63) and (112) that the first-order flattening function F_1 is a constant. It has the value F_{1B} everywhere in the core and its derivative is zero within the core. This simplifies the other ODE of (63) considerably. The equation for K_2 is

$$\beta^2 K_2'' + 6\beta K_2' - 14 K_2 = 0 \tag{74}$$

The boundary conditions on (74) are that K_2 is finite at the origin and that it is equal to K_{2B} on the core-envelope boundary. The solution to (74) and the boundary condition at β equal to β_C are

$$\begin{aligned} K_2 &= K_{2B}\left(\frac{\beta}{\beta_C}\right)^2 \\ K'_{2B} &= 2\left(\frac{K_{2B}}{\beta_C}\right) \end{aligned} \tag{75}$$

Both the shape functions and their first derivatives are continuous at the core-envelope boundary. Therefore, the above boundary condition applies to both the core and the envelope at β equal to β_C. Similarly, the equation for F_2 from (63) and (112) is

$$\beta^2 F''_2 + 6\beta F'_2 = -8K_2 \tag{76}$$

with the solution

$$\begin{aligned} F_2 &= F_{2B} + \frac{4}{7}K_{2B}\left[1 - \left(\frac{\beta}{\beta_C}\right)^2\right] \\ F'_{2B} &= -\frac{8}{7}\left(\frac{K_{2B}}{\beta_C}\right) \end{aligned} \tag{77}$$

The equation for H_3 is

$$\beta^2 H''_3 + 6\beta H'_3 - 36H_3 = -88\left(\frac{\beta}{\beta_C}\right)^2 F_{1B}K_{2B} \tag{78}$$

with solution

$$\begin{aligned} H_3 &= H_{3B}\left(\frac{\beta}{\beta_C}\right)^4 + 4F_{1B}K_{2B}\left(\frac{\beta}{\beta_C}\right)^2\left[1 - \left(\frac{\beta}{\beta_C}\right)^2\right] \\ H'_{3B} &= 4\left(\frac{H_{3B}}{\beta_C}\right) - 8\left(\frac{F_{1B}K_{2B}}{\beta_C}\right) \end{aligned} \tag{79}$$

The equation for K_3 is

$$\beta^2 K''_3 + 6\beta K'_3 - 14K_3 = 48\left(\frac{\beta}{\beta_C}\right)^4 F_{1B}K_{2B} - 12\left(\frac{\beta}{\beta_C}\right)^4 H_{3B} \tag{80}$$

with solution

$$\begin{aligned} K_3 &= K_{3B}\left(\frac{\beta}{\beta_C}\right)^2 - \frac{24}{11}F_{1B}K_{2B}\left(\frac{\beta}{\beta_C}\right)^2\left[1 - \left(\frac{\beta}{\beta_C}\right)^2\right] + \frac{6}{11}H_{3B}\left(\frac{\beta}{\beta_C}\right)^2\left[1 - \left(\frac{\beta}{\beta_C}\right)^2\right] \\ K'_{3B} &= 2\left(\frac{K_{3B}}{\beta_C}\right) + \frac{48}{11}\left(\frac{F_{1B}K_{2B}}{\beta_C}\right) - \frac{12}{11}\left(\frac{H_{3B}}{\beta_C}\right) \end{aligned} \tag{81}$$

Finally, the equation for F_3 is

$$\begin{aligned} \beta^2 F''_3 + 6\beta F'_3 = &\frac{8}{385}\left(\frac{\beta}{\beta_C}\right)^2\left[2039 - 3150\left(\frac{\beta}{\beta_C}\right)^2\right]F_{1B}K_{2B} \\ &-\frac{12}{11}\left(\frac{\beta}{\beta_C}\right)^2\left[4 - 15\left(\frac{\beta}{\beta_C}\right)^2\right]H_{3B} - 8\left(\frac{\beta}{\beta_C}\right)^2 K_{3B} \end{aligned} \tag{82}$$

with solution

$$
\begin{aligned}
F_3 = & F_{3B} - F_{1B}K_{2B}\left[1-\left(\frac{\beta}{\beta_C}\right)^2\right]\left[\frac{296}{245}-\frac{20}{11}\left(\frac{\beta}{\beta_C}\right)^2\right] \\
& -H_{3B}\left[1-\left(\frac{\beta}{\beta_C}\right)^2\right]\left[\frac{1}{7}+\frac{5}{11}\left(\frac{\beta}{\beta_C}\right)^2\right]+\frac{4}{7}K_{3B}\left[1-\left(\frac{\beta}{\beta_C}\right)^2\right] \\
F'_{3B} = & -\frac{3288}{2695}\left(\frac{F_{1B}K_{2B}}{\beta_C}\right)+\frac{92}{77}\left(\frac{H_{3B}}{\beta_C}\right)-\frac{8}{7}\left(\frac{K_{3B}}{\beta_C}\right)
\end{aligned}
\tag{83}
$$

5.8 Solution to the Theory of Figures in a Constant-Density Envelope

When the normalized envelope density δ_E is a constant, (73) yields the following expression for the normalized density in the core

$$\delta_C = \delta_E + \frac{1-\delta_E}{\beta_C^3} \tag{84}$$

The gravitational moment S_0 in the envelope is similarly

$$S_0 = \delta_E + \frac{1-\delta_E}{\beta^3} \tag{85}$$

A value for δ_E, and also S_0 from (85), can be substituted into the differential equations given by (63) and (112), and the solution for the spheroidal functions in the envelope can be found subject to the boundary conditions at the surface, given in Sec. 5.3, and the boundary conditions at normalized radius β_C given by expressions at the core boundary in Sec. 5.7. The normalized core radius β_C enters through the boundary conditions of Sec. 5.7 only. For any finite value of δ_E the solutions to the ODE are complicated and lengthy, although solutions do exist for the two-zone model considered here. Nevertheless, beyond this idealized two-zone model, numerical integration is required when the envelope density varies with β. Perhaps the exact solutions to the ODE for constant density are useful for purposes of checking the precision of the numerical integration, but they have no particular advantage to the problem of interior modeling. In practice, numerical integration is a useful general approach for any envelope density, including constant density. The precision of the numerical integration can be adjusted such that it is competitive with the exact solutions to the constant-density envelope, especially given the limited accuracy required by the observational constraints.

However, the exact solution is tractable for the case where the density in the envelope is zero. This is the generalized Roche model considered by Zharkov and Trubitsyn (1978) and discussed in Section 4. The envelope contains no gravitational mass contribution to the HE, but there is an inertial contribution from the centrifugal potential, and hence a contribution to the surface shape of the planet. For purposes of illustrating the ODE approach, we solve this Roche case in section 5.8.1 and finally consider the general case of finite density in section 5.8.2.

5.8.1 The Generalized Roche Model

For δ_E equal to zero, the density of material in the core is given by ρ_0/β_C^3. In turn, the differential equation for F_1 in the envelope becomes

$$\beta^2 F_1'' - 6F_1 = 0 \tag{86}$$

The boundary conditions on the solution for F_1 is that $F_1' = 5/2 - 2F_1$ at β equal to one, and F_1' equal to zero at β equal to β_C. With these boundary conditions, F_1 in the envelope is given by

$$\begin{aligned} F_1 &= \frac{2\beta^5 + 3\beta_C^5}{4\beta^2} \\ F_1' &= \frac{3\left(\beta^5 - \beta_C^5\right)}{2\beta^3} \\ F_{11} &= \frac{1}{4}\left(2 + 3\beta_C^5\right) \\ F_{1B} &= \frac{5}{4}\beta_C^3 \end{aligned} \tag{87}$$

Here F_{11} is the value of F_1 at the surface, and F_{1B} is the value of F_1 at the core boundary. All the quantities in (87) are needed for solutions to the ODE for the higher order shape functions. The value of F_1 in the core is determined by the envelope density distribution, which in this Roche case is zero, but it is true in general for any envelope density distribution. For the Roche model, the density distribution in the core is simply a constant, given by F_{1B} according to the core solution of Sec. 5.7.

The differential equation for the function K_2 is obtained from (63) and (112), and after the envelope density is set to zero and the solution for F_1 is inserted into G_{42}, the equation for the Roche model is

$$\beta^2 K_2'' - 20K_2 = \frac{15}{16}\beta\left(\beta^5 + 4\beta_C^5\right) \tag{88}$$

Again, with the boundary conditions from Sections 5.3 and 5.7, the solution for K_2 is

$$\begin{aligned} K_2 &= \frac{3}{32}\frac{\left(\beta^5 - \beta_C^5\right)^2}{\beta^4} \\ K_2' &= \frac{3}{16}\frac{\left(3\beta^{10} - \beta^5\beta_C^5 - 2\beta_C^{10}\right)}{\beta^5} \\ K_{21} &= \frac{3}{32}\left(1 - \beta_C^5\right)^2 \\ K_{2B} &= 0 \end{aligned} \tag{89}$$

Similarly, the differential equation for F_2 is

$$\beta^2 F_2'' - 6F_2 = -\frac{3\beta_C^5}{16\beta^4}\left(4\beta^5 + 11\beta_C^5\right) \tag{90}$$

and the solution is

$$
\begin{aligned}
F_2 &= \frac{\beta_C^5}{224\beta^4}\left(28\beta^5 + 80\beta^2\beta_C^3 - 33\beta_C^5\right) \\
F_2' &= \frac{\beta_C^5}{56\beta^5}\left(7\beta^5 - 40\beta^2\beta_C^3 + 33\beta_C^5\right) \\
F_{21} &= \frac{\beta_C^5}{224}\left(28 + 80\beta_C^3 - 33\beta_C^5\right) \\
F_{2B} &= \frac{75\beta_C^6}{224}
\end{aligned}
\tag{91}
$$

This process can be extended to third order, although the expressions for H_3, K_3 and F_3 as a function of β in the envelope become more lengthy. We list here only their values at the surface, which are

$$
\begin{aligned}
H_{31} &= \frac{1}{160}\left(1-\beta_C^5\right)^2\left(38+67\beta_C^5\right) \\
K_{31} &= -\frac{1}{2240}\left(42+49\beta_C^5+200\beta_C^8-424\beta_C^{10}-200\beta_C^{13}+333\beta_C^{15}\right) \\
F_{31} &= \frac{1}{94080}\left(7056+392\beta_C^5+5600\beta_C^8-462\beta_C^{10}+74000\beta_C^{11}-13200\beta_C^{13}-4011\beta_C^{15}\right)
\end{aligned}
\tag{92}
$$

The values for the gravitational coefficients can be obtained from (72). The results are

$$
\begin{aligned}
J_{21} &= \frac{1}{2}\beta_C^5 \\
J_{22} &= -\frac{1}{2}\beta_C^5\left(\frac{1}{3} - \frac{10}{21}\beta_C^3 + \frac{1}{2}\beta_C^5\right) \\
J_{23} &= -\frac{1}{2}\beta_C^5\left(\frac{23}{180} + \frac{10}{63}\beta_C^3 - \frac{1}{30}\beta_C^5 - \frac{925}{882}\beta_C^6 + \frac{10}{21}\beta_C^8 + \frac{9}{140}\beta_C^{10}\right) \\
J_{42} &= -\frac{15\beta_C^{10}}{28} \\
J_{43} &= \frac{15\beta_C^{10}}{28}\left(\frac{2}{3} - \frac{20}{21}\beta_C^3 + \beta_C^5\right) \\
J_{63} &= \frac{125}{168}\beta_C^{15}
\end{aligned}
\tag{93}
$$

These results for the gravitational coefficients in the generalized Roche model agree with Zharkov and Trubitsyn (1978), except for J_{23}. Total agreement is a good check on our ODE method, as the derivation in Zharkov and Trubitsyn (1978) is quite different from ours. We suggest that the third order term for J_2 in Zharkov and Trubitsyn (1978) contains typographical errors. For example, by setting the core radius to one in (93), the case of a constant-density planet is recovered. The result is

$$
\begin{aligned}
J_2 &= \frac{1}{2}m - \frac{5}{28}m^2 + \frac{25}{196}m^3 \\
J_4 &= -\frac{15}{28}m^2 + \frac{75}{196}m^3 \\
J_6 &= \frac{125}{168}m^3
\end{aligned}
\tag{94}
$$

This is correct (Zharkov and Trubitsyn, 1978), and it is a good check on the ODE method. However, if β_C is set equal to one in (34.6) for J_2 in Zharkov and Trubitsyn (1978), the result is $J_2 = (1/2)m - (5/28)m^2 - (1889/4410)m^3$. This is not correct. We conclude that there is agreement between our ODE method and the method of Zharkov and Trubitsyn, but only if the third order J_2 term in Zharkov and Trubitsyn (1978) is brought into agreement with J_{23} in (93).

Although the generalized Roche model is an idealization of a real giant planet, it illustrates the method. Starting with a density distribution in the envelope given by $\delta_E(\beta)$ and a core radius β_C, the zonal gravitational coefficients in the external gravitational potential can be calculated. In general, the results are obtained by numerical integration of the ODE, but the numerical values analogous to the six functions of (93) can be calculated to any arbitrary precision. A comparison of the calculated values with the measured values is achieved by calculating the value of the small rotational parameter m for the planet in question, and then by applying (69).

5.8.2 Model for a Finite-Density Envelope

Even for this simple case of a finite-density envelope, the solution to the ODE can be obtained by numerical integration. For purposes of illustrating the method, we pick a normalized envelope density of 1/2 and a normalized core radius of 1/2. By (73) the density δ_C in the core is equal to 9/2, and the percentage of the total mass in the core ($\delta_C \beta_C^3$) is 9/16. This particular choice of δ_E and β_C results in a fairly simple differential equation for the first-order function F_1. By (63) we have

$$\beta^2 \left(1 + \beta^3\right) F_1'' + 6\beta^4 F_1' - 6F_1 = 0 \tag{95}$$

The integration can be done numerically subject to the boundary conditions of sections 5.3 and 5.7, which for $F_1(\beta)$ are

$$\begin{aligned} F_1'(1) &= \frac{5}{2} - 2F_1(1) \\ F_1'(\beta_C) &= 0 \end{aligned} \tag{96}$$

The limits of integration are from β_C to one. After the numerical integration is complete, a value of F_1 anywhere on the interval $\beta_C \leq \beta \leq 1$ can be found by numerical interpolation. This solution in the envelope can be matched to the solution in the core given in Sec. 5.7. A plot of this particular case throughout the interior is shown in Fig. 3.

Because the differential equation for K_2 involves both F_1 and its first derivative, it must be evaluated numerically by interpolating in the numerical solution to (95). Furthermore, the boundary condition at the surface is not known until F_1 at the surface is known. Therefore, we do not write down the differential equation that must be integrated, but instead numerically evaluate it according to (63) on the interval

$\beta_C \leq \beta \leq 1$. The boundary conditions for this special case, with δ_E and β_C both equal to 1/2, are obtained from the expressions given in Sec. 5.3 and Sec. 5.7, and include the solution for F_1 at the surface. In general, the boundary conditions are

$$\begin{aligned} K_2'(\beta_C) &= 2\left(\frac{K_2(\beta_C)}{\beta_C}\right) \\ K_2'(1) &= \frac{25}{16} - \frac{5}{4}F_1(1) - 4K_2(1) \end{aligned} \tag{97}$$

and by numerical interpolation in the previous solution, $F_1(1)$ is equal to 99060576/131853043, accurate to 16 places past the decimal. With these boundary conditions, numerical integration yields the solution for K_2 in the envelope, which can be matched to the core solution and plotted. The result is shown in Fig. 4.

The procedure is similar for the function F_2, and the differential equation from (63) involves the previous solution for both F_1 and K_2 and their first derivatives. The boundary conditions are

$$\begin{aligned} F_2'(\beta_C) &= -\frac{8}{7}\left(\frac{K_2(\beta_C)}{\beta_C}\right) \\ F_2'(1) &= -\frac{5}{12} + \frac{19}{42}F_1(1) + \frac{1}{3}F_1(1)^2 + \frac{8}{7}K_2(1) - 2F_2(1) \end{aligned} \tag{98}$$

where for this special case, $K_2(1/2)$ is equal to 143636/109713139 and $K_2(1)$ is equal to 6168175/61992373, again accurate to 16 places past the decimal. After numerical integration, the solution for F_2 is represented by Fig. 5.

The above process can be repeated for the third-order functions H_3, K_3 and F_3, in that order. As each function is introduced, all previous solutions are used in both the ODE and in the boundary conditions. The results for the special case considered here are represented by Fig. 6, Fig. 7 and Fig. 8. All six plotted functions can be evaluated at the surface. As a result, the shape of the surface is given by (32) with β equal to one and with

$$\begin{aligned} f_1 &= \frac{1424483}{1896036}m + \frac{8128}{132573}m^2 + \frac{14522}{96145}m^3 \\ k_1 &= \frac{9750}{97991}m^2 - \frac{139}{46715}m^3 \\ h_1 &= \frac{49427}{155163}m^3 \end{aligned} \tag{99}$$

These expressions for f, k, and h at the surface are accurate to 10 significant digits. For all practical purposes they are limited only by the uncertainty in the small rotational parameter m, and of course by truncation of the series at order m^3. Similarly, by (72), the surface conditions can be used to calculate the gravitational coefficients in the external potential. The results for this special case are

$$\begin{aligned} J_2 &= \frac{156041}{931420}m - \frac{980}{25913}m^2 + \frac{339}{46459}m^3 \\ J_4 &= -\frac{6381}{56362}m^2 + \frac{2864}{63535}m^3 \\ J_6 &= \frac{5277}{46804}m^3 \end{aligned} \tag{100}$$

6 Application to Planets

In this section we apply the two-layer model of this paper (with constant core and envelope densities) to the planets. The model is a simple one for planets, and it is most applicable to terrestrial planets and icy satellites that have a differentiated structure consisting of either a metallic core and a rocky mantle or a rock, metal core and an icy mantle. Application to the gas and ice giant planets will also be made, though a constant-density envelope is not a very realistic model of these bodies. However, with some generalization of the two-layer model to include envelopes with arbitrary radial density profiles, application to giant planets can be made much more realistic. The approximate theory of figures approach presented in this paper is readily generalized to arbitrary radial density profiles in the envelope, and the exact solution can also be extended to this case.

6.1 Earth

Table 3 presents the eccentricities and gravitational coefficient J_2 for a two-layer model of the Earth with parameters $\rho_2/\rho_1 = 0.401$, $Q_{\rm V} = 0.1674$, and $\epsilon_2 = 0.002$. Results are given for the exact solution to the two-layer problem and for the theory of figures. Approximate solutions are valid to orders 1, 2, and 3 in the small parameter m. Table 3 also lists the observed values of E_1, E_2, and J_2. Two-layer models provide a good match to the observed eccentricities and an acceptable match to the gravitational coefficient. No attempt was made to fine tune the model parameters. For this case, even the theory of figures to first order in m gives good agreement with the exact solution and with the observations.

6.2 Mars

Table 4 gives results for a Mars model with $\rho_2/\rho_1 = 0.486$, $Q_V = 0.125$, $\epsilon_2 = 0.00347$. There are no observations of the eccentricity of the Martian core-mantle boundary. The models provide good estimates of the eccentricity of the surface and the theory of figures approximations match the exact solution of E_2 quite closely. The eccentricity of the core-mantle boundary is less than that of the surface, as was the case for the Earth models, and E_1 from the theory of figures approximations agrees rather well with the value of E_1 from the exact solution. The model J_2 is not in particularly good agreement with the observed J_2 for Mars, but it is emphasized that we made no attempt to fine tune the model parameters to fit J_2. Moreover, the radius of the Martian core and the densities of the Martian core and mantle are not known.

6.3 Neptune

Table 5 lists results for a Neptune model with $\rho_2/\rho_1 = 0.157334$, $Q_{\rm V} = 0.091125$. $\epsilon_2 = 0.0254179$ (parameter values based on a model in C.Z. Zhang (1997)). It is emphasized that the two-layer model with a constant-

density envelope is not a good model for an ice giant planet like Neptune. Nevertheless, the shape of the surface is not too different from Neptune's observed shape, but J_2 for the model is almost a factor of 2 larger than the observed value. We do not know if Neptune has a core-envelope configuration or a continuous radial density profile.

6.4 Uranus

Table 6 provides results for two Uranus models with model parameters given in the table and based on Horedt and Hubbard (1983). As was the case for Neptune, the Uranus models do okay in matching E_2 but fail to give good estimates for J_2. Similar to Neptune, it is not known if the radial density profile of Uranus is a smooth one or if it contains a discontinuity associated with a core.

7 Discussion and Conclusions

The exact solution for the rotational distortion of a two-layer Maclaurin ellipsoid reported in Kong et al. (2010) has been extended here to provide formulas for the standard spherical harmonic expansion of the external gravitational field of the body. We have also presented a new approach to the evaluation of the theory of figures based on numerical integration of ordinary differential equations.

The classical Radau-Darwin formula is a low order result from the theory of figures and its realm of validity has been evaluated for the two-layer model using the exact solution. It was found that the Radau-Darwin approximation is not valid for the rotational parameter $\epsilon_2 = \Omega^2/(2\pi \mathrm{G}\rho_2) \geq 0.17$ since the formula predicts a surface eccentricity that is smaller than the eccentricity of the core-envelope boundary. Interface eccentricity must be smaller than surface eccentricity. For an envelope density of 3000 kg m^{-3} the failure of the Radau-Darwin formula corresponds to a rotation period of about 3 hr.

The generalized Roche model, a two-layer model with an envelope density equal to zero, provides a simple model against which to evaluate the validity of the theory of figures against the exact solution. It was found that the theory of figures only slightly underestimates the eccentricities of the surface and core-envelope interface compared with the exact solution.

Application of the exact solution and the theory of figures is made to models of Earth, Mars, Uranus, and Neptune. It is found that the two-layer model with constant densities in the layers can provide realistic approximations to terrestrial planets and icy outer planet satellites. This is perhaps not surprising since the zeroth order structure of these planetary bodies is similar to the two-layer model with constant densities in the layers. The situation is not as straightforward for giant planets since a constant density envelope is not a particularly good representation of the density in the outer layers of such planets. However, the theory of figures, as developed in this paper, is readily generalized to models with arbitrary radial density profiles in

the envelope (though we have not carried this out in this paper). Such models will be particularly useful for Jupiter and Saturn which might possess heavy element cores surrounded by gaseous envelopes. The envelope density can be represented by polynomial functions of radius. Inversions of gravitational data based on these models provide constraints on the gas giant interiors independent of assumptions about composition and equations of state. The exact solution for the two-layer Maclaurin ellipsoid can also be extended to allow for a non-constant radial profile of envelope density. This is not as straightforward as the generalization of the theory of figures, but it can be done. The solutions for two-layer bodies can therefore provide acceptable models for the rotational distortion of terrestrial, gas giant, and ice giant planetary bodies. These solutions can also serve as benchmarks to test the validity of complicated numerical models that invert gravitational and shape data to infer the interior structure of planets.

References

Anderson, J. D., Schubert, G., 2007. Saturn's gravitational field, internal rotation, and interior structure. Science 317, 1384–1387, doi:10.1126/science.1144835.

Chandrasekhar, S., 1969. Ellipsoidal Figures of Equilibrium. The Silliman Foundation Lectures. Yale University Press, New Haven, CT.

Darwin, G. H., 1900. The Theory of the Figure of the Earth Carried to the Second Order of Small Quantities. Mon. Not. Roy. Astron. Soc. 60, 82–124.

Gundlach, J. H., Merkowitz, S. M., 2000. Measurement of Newton's constant using a torsion balance with angular acceleration feedback. Phys. Rev. Lett. 85, 2869–2872, doi:10.1103/PhysRevLett.85.2869.

Horedt, G. P., Hubbard, W. B., 1983. Two- and three-layer models of Uranus. Earth Moon Planets 29, 229–236.

Jacobson, R. A., 2007. The gravity field of the Uranian system and the orbits of the Uranian satellites and rings. Bull. Amer. Astron. Soc. 39, 453.

Jacobson, R. A., 2009. The orbits of the Neptunian satellites and the orientation of the pole of Neptune. Astron. J. 137, 4322–4329, doi:10.1088/0004–6256/137/5/4322.

Kaula, W. M., 1968. An Introduction to Planetary Physics: The Terrestrial Planets. John Wiley & Sons, Inc., New York, N.Y.

Kong, D., Zhang, K., Schubert, G., 2010. Shapes of two-layer models of rotating planets. J. Geophys. Res. 115, doi:10.1029/2010JE003720.

Lamb, H., 1932. Hydrodynamics. Cambridge University Press, Cambridge, UK.

Lindal, G. F., 1992. The atmosphere of Neptune - an analysis of radio occultation data acquired with Voyager 2. Astron. J. 103, 967–982.

Radau, R., 1885. Sur la loi des densités à l'intérieur de la terre. Comptes Rendu 100, 972–974.

Zhang, C. Z., 1997. Uranus and Neptune models. Earth Moon Planets 75, 17–24.

Zharkov, V. N., Trubitsyn, V. P., 1976. Fifth-approximation system of equations for the theory of figure. Soviet Astron. 19, 366–372.

Zharkov, V. N., Trubitsyn, V. P., 1978. Physics of Planetary Interiors. W. B. Hubbard, ed., Pachart Press, Tucson, AZ.

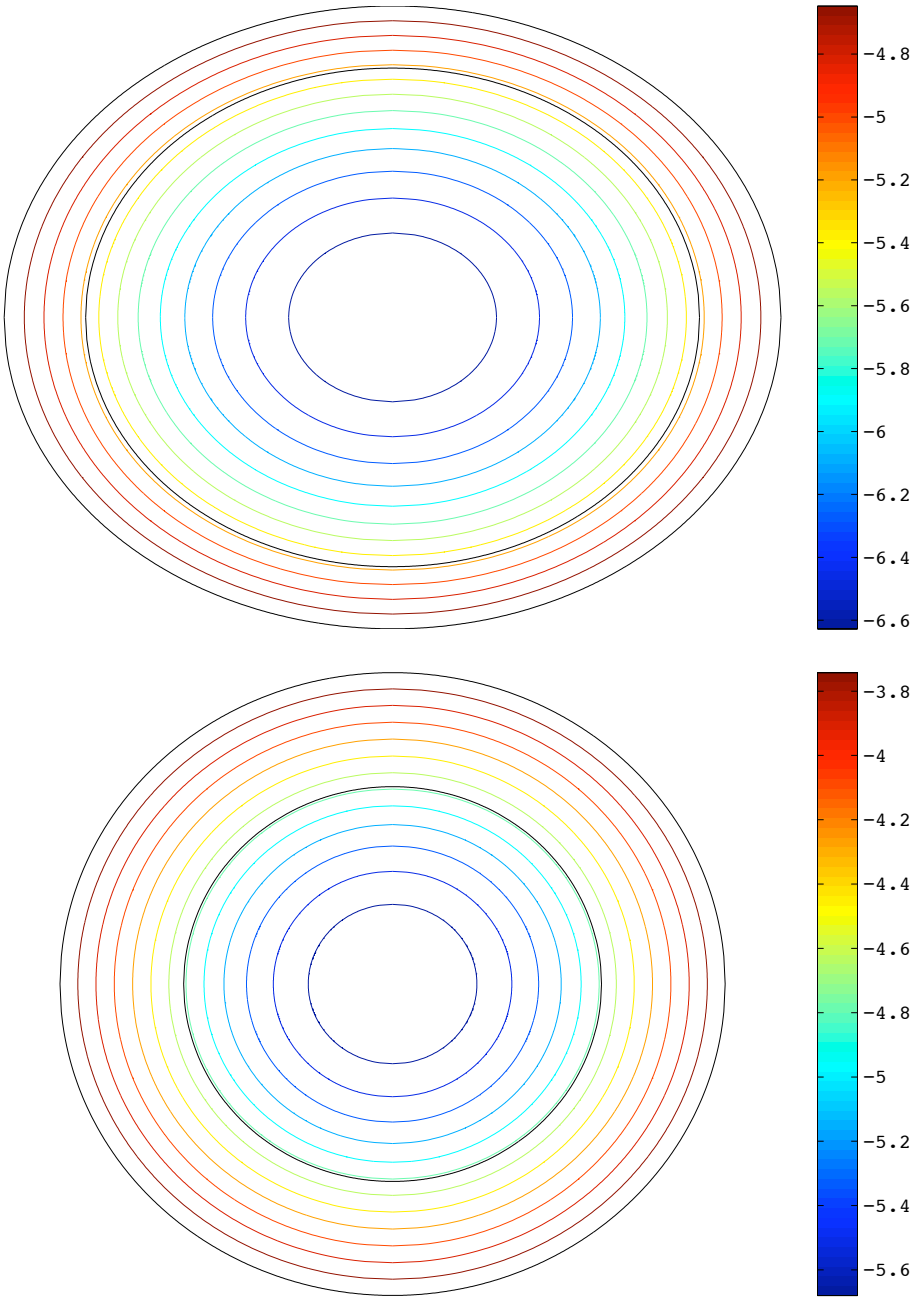

Figure 1: Surfaces of constant total (gravity) potential for cases (a) $Q_{\mathrm{V}} = 0.5$, $\rho_1/\rho_2 = 2$, $\epsilon_2 = 0.18$ and (b) $Q_{\mathrm{V}} = 0.25$, $\rho_1/\rho_2 = 2$, $\epsilon_2 = 0.05$.

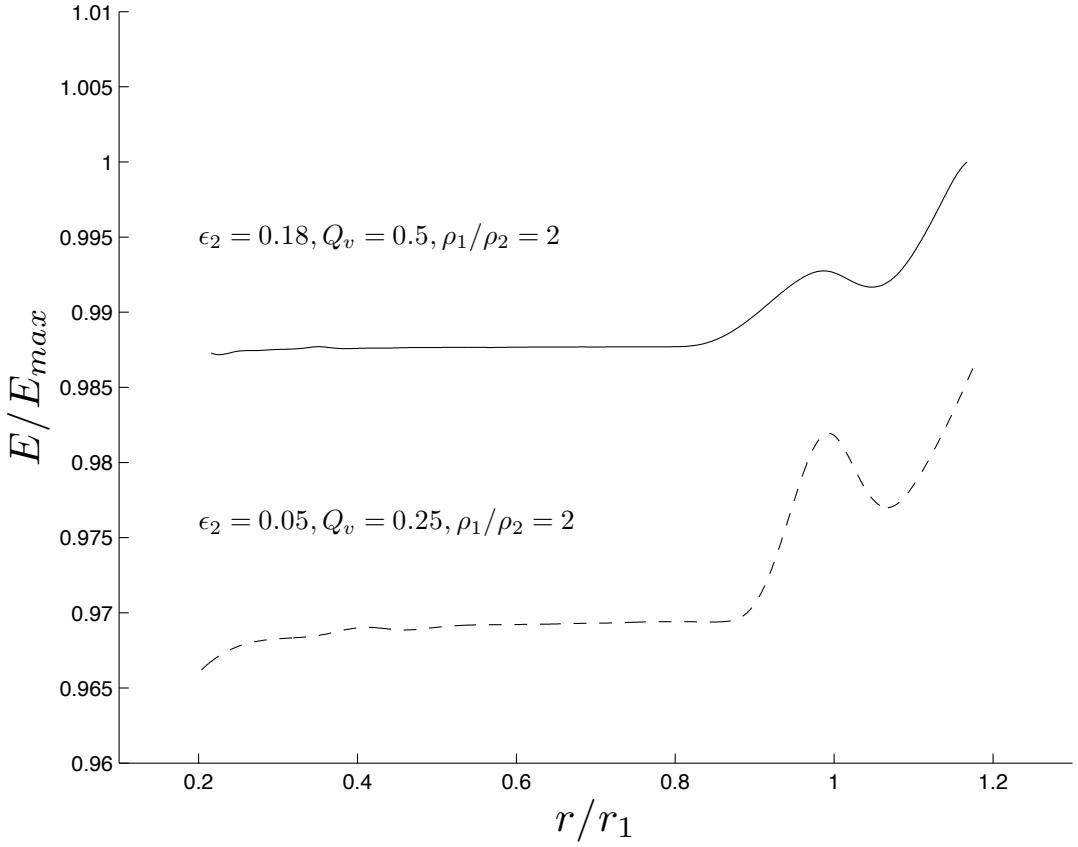

Figure 2: The eccentricity of the total potential isosurfaces in Fig. 1 plotted as a function of radius.

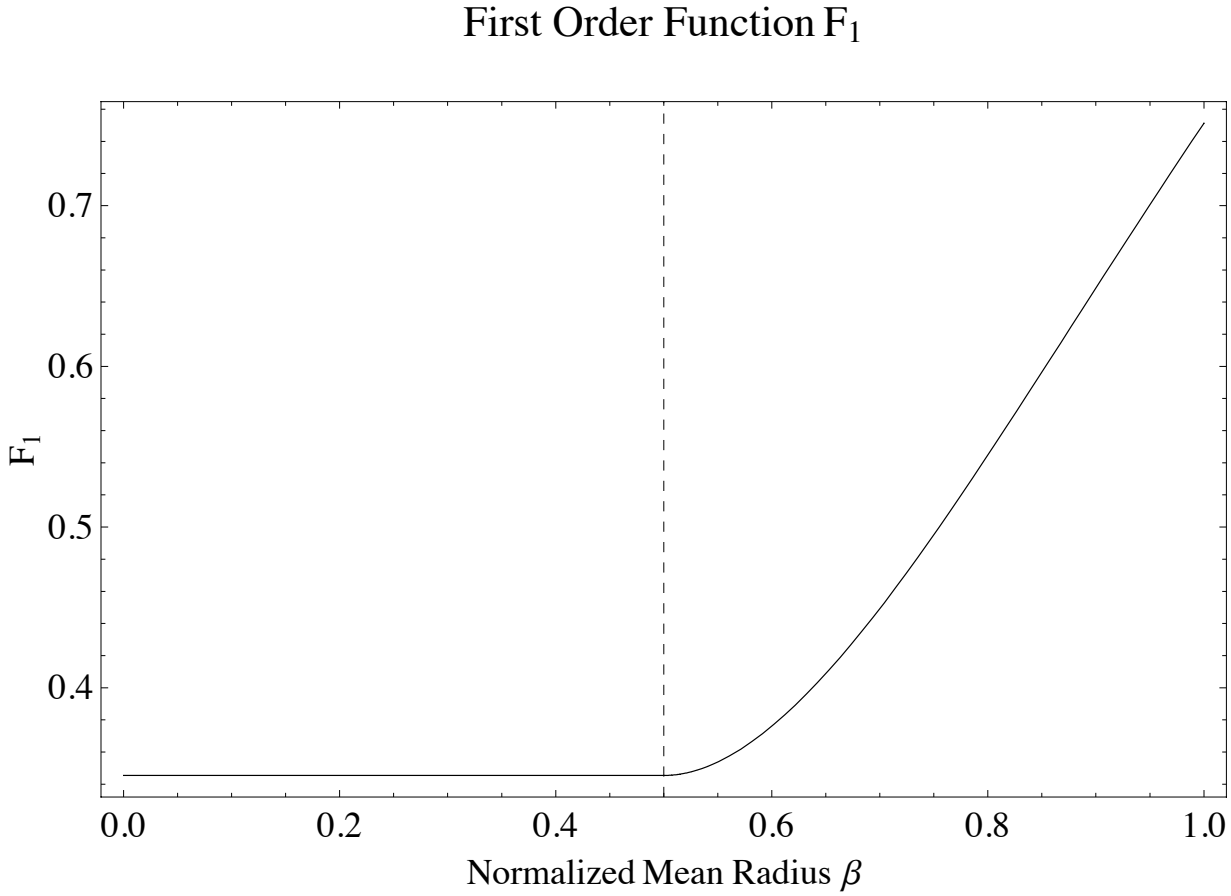

Figure 3: Function $F_1(\beta)$ for normalized envelope density δ_E of 0.5 and core radius β_C of 0.5.

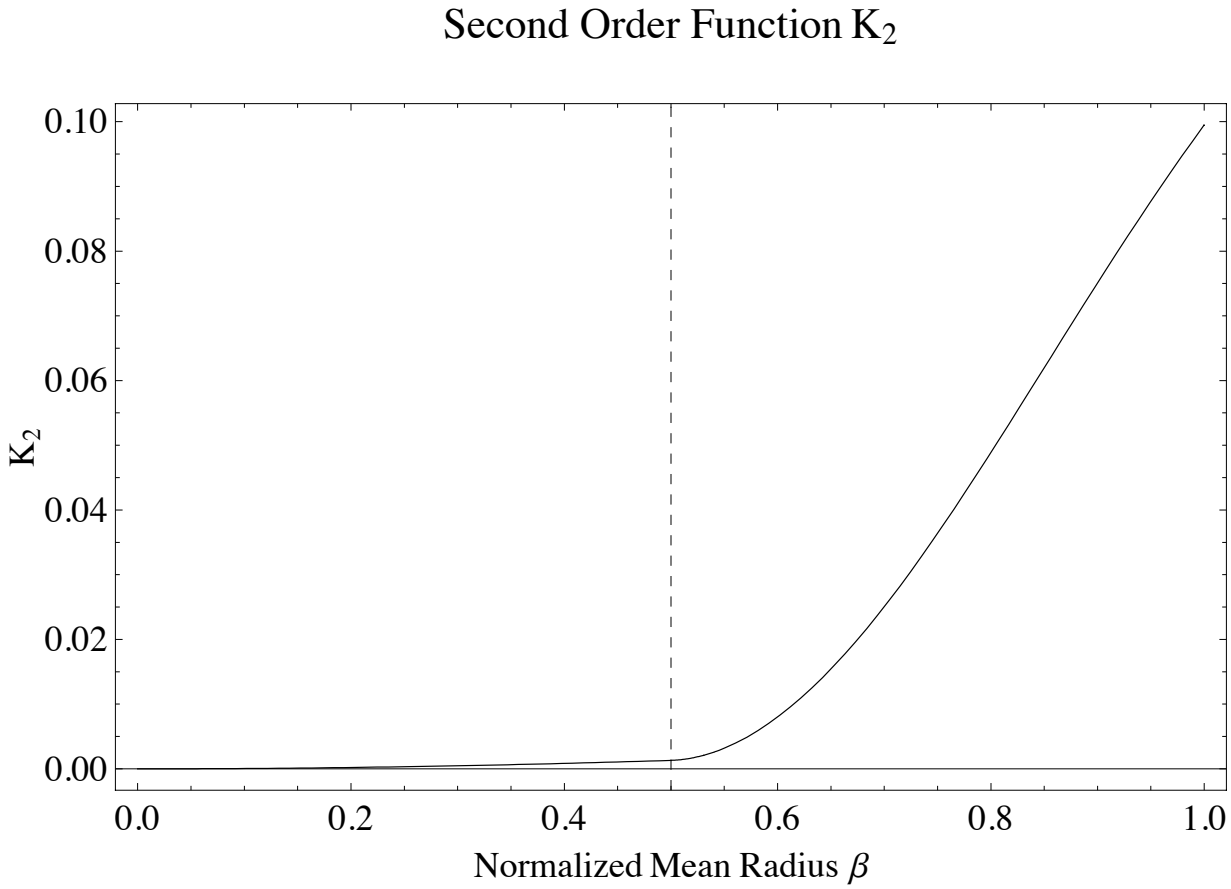

Figure 4: Function $K_2(\beta)$ for normalized envelope density δ_E of 0.5 and core radius β_C of 0.5.

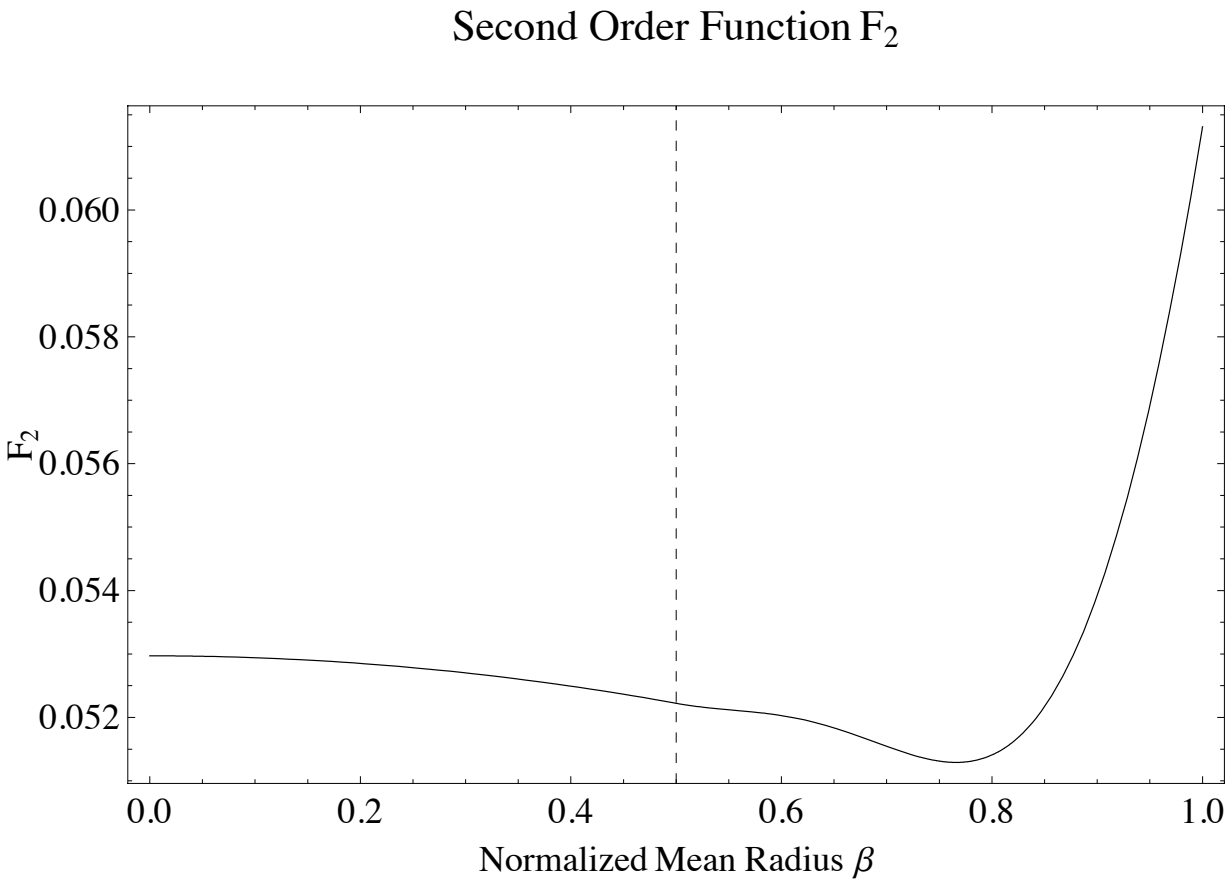

Figure 5: Function $F_2(\beta)$ for normalized envelope density δ_E of 0.5 and core radius β_C of 0.5.

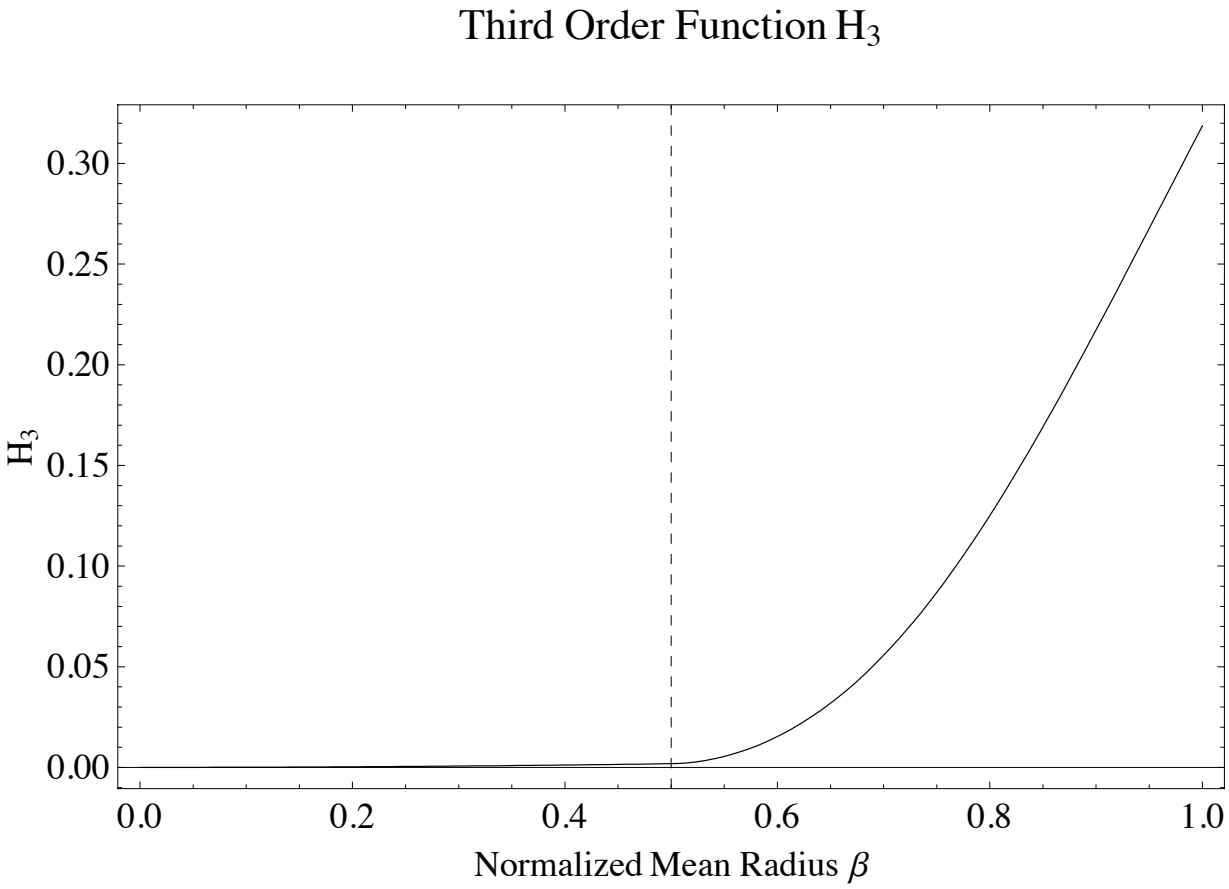

Figure 6: Function $H_3(\beta)$ for normalized envelope density δ_E of 0.5 and core radius β_C of 0.5.

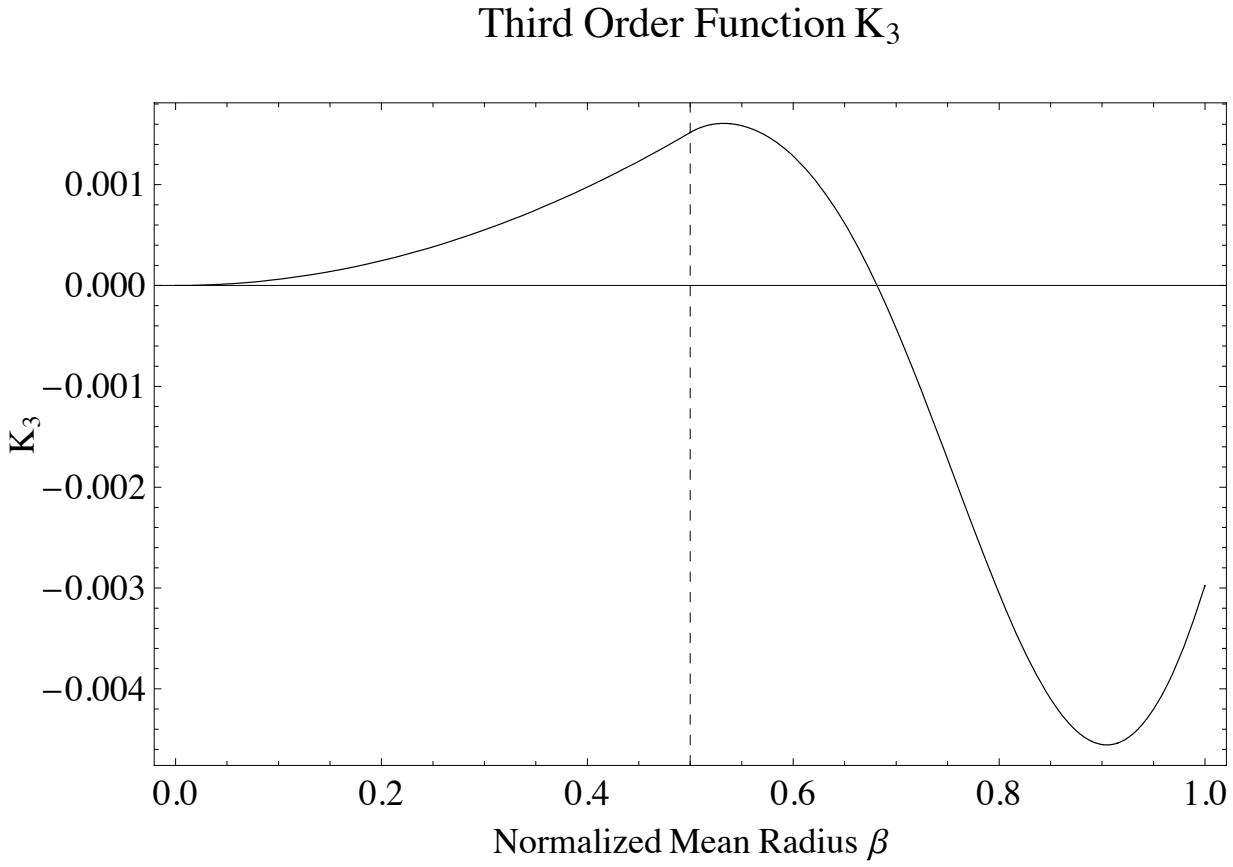

Figure 7: Function $K_3(\beta)$ for normalized envelope density δ_E of 0.5 and core radius β_C of 0.5.

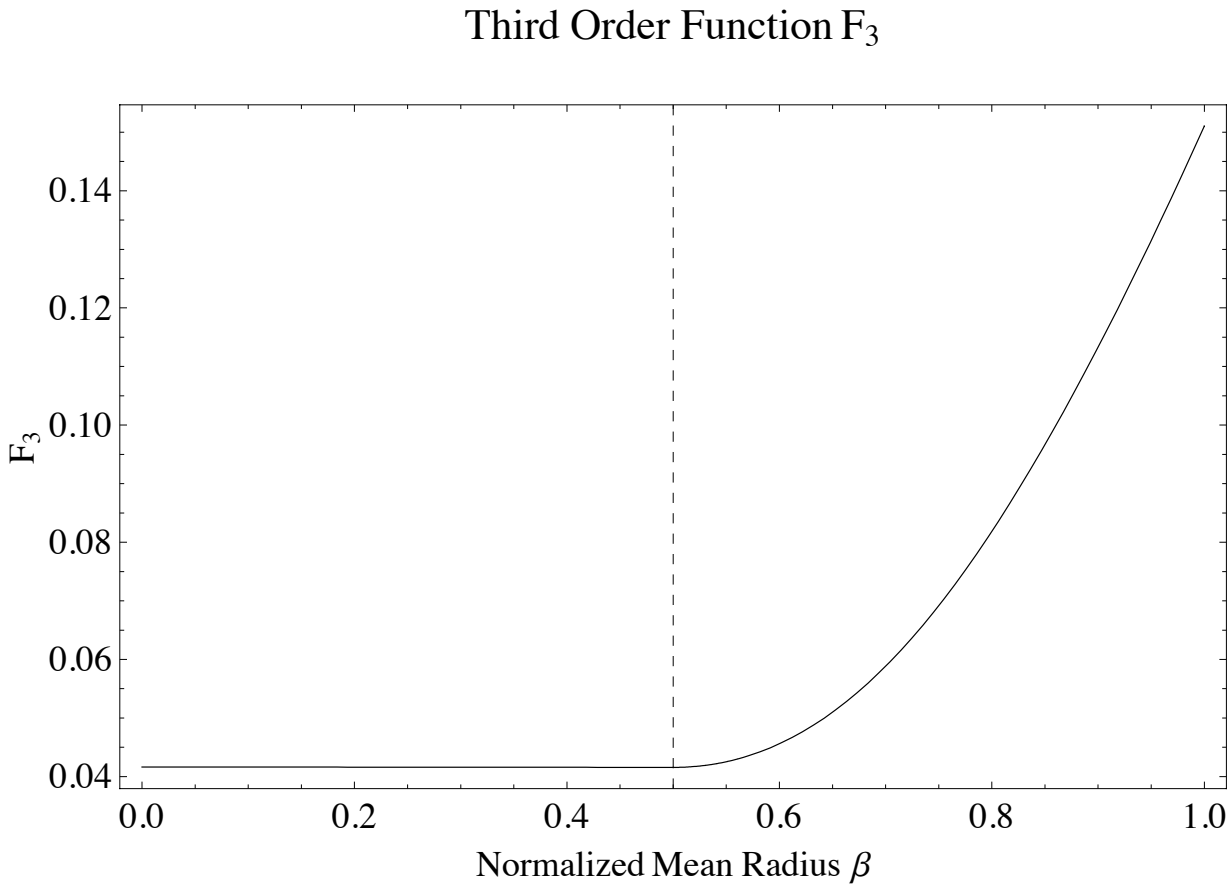

Figure 8: Function $F_3(\beta)$ for normalized envelope density δ_E of 0.5 and core radius β_C of 0.5.

Table 1: Eccentricities of the interface E_1 and the surface E_2 as a function of the rotation parameter ϵ_2 for $Q_{\rm V} = 0.5$ and $\rho_1/\rho_2 = 2$. The surface eccentricity based on the Radau-Darwin approximation is E_2^{R-D}.

ϵ_2	E_1	E_2	E_2^{R-D}
0.01000	0.13959	0.14390	0.14383
0.02000	0.19761	0.20330	0.20288
0.03000	0.24158	0.24860	0.24782
0.04000	0.27886	0.28670	0.28540
0.05000	0.31147	0.32010	0.31824
0.06000	0.34050	0.35010	0.34769
0.07000	0.36770	0.37770	0.37453
0.08000	0.39250	0.40320	0.39931
0.09000	0.41592	0.42710	0.42238
0.10000	0.43790	0.44960	0.44402
0.11000	0.45864	0.47090	0.46441
0.12000	0.47895	0.49130	0.48372
0.13000	0.49789	0.51070	0.50208
0.14000	0.51604	0.52930	0.51957
0.15000	0.53399	0.54730	0.53630
0.16000	0.55103	0.56460	0.55232
0.17000	0.56739	0.58130	0.56771
0.18000	0.58335	0.59750	0.58250
0.19000	0.59873	0.61320	0.59674
0.20000	0.61401	0.62854	0.61047
0.21000	0.62897	0.64350	0.62373
0.22000	0.64315	0.65800	0.63654
0.23000	0.65732	0.67224	0.64894
0.24000	0.67128	0.68620	0.66093

Table 2: Comparison of interface and surface eccentricities for several models with small envelope densities computed from the exact theory and the theory of figures Roche model evaluated to second order in m.

ρ_2/ρ_1	$\epsilon_2\rho_2/\rho_1$	Q_v	E_1	E_2	$E_1^{\rm ToF}(\rho_2=0)$	$E_2^{\rm ToF}(\rho_2=0)$
10^{-2}	0.05	0.5	0.4297	0.4629	0.4268	0.4603
10^{-3}	0.05	0.5	0.4292	0.46296	0.4268	0.4603
10^{-4}	0.05	0.5	0.4291	0.46296	0.4268	0.4603
10^{-2}	0.05	0.33	0.4378	0.5189	0.4268	0.5141
10^{-3}	0.05	0.33	0.4366	0.5195	0.4268	0.5141
10^{-4}	0.05	0.33	0.4365	0.51955	0.4268	0.5141
10^{-2}	0.02	0.5	0.2730	0.2953	0.2724	0.2949
10^{-3}	0.02	0.5	0.27297	0.29537	0.2724	0.2949
10^{-4}	0.02	0.5	0.2728	0.29537	0.2724	0.2949
10^{-2}	0.02	0.33	0.2757	0.3314	0.2724	0.3313
10^{-3}	0.02	0.33	0.2749	0.3318	0.2724	0.3313
10^{-4}	0.02	0.33	0.2748	0.3318	0.2724	0.3313

Table 3: Application of exact solution and theory of figures to Earth.
Two-layer Earth model: $\rho_2/\rho_1 = 0.401$, $Q_{\rm V} = 0.1674$, $\epsilon_2 = 0.002$.

	1st order	2nd order	3rd order	exact	observed
E_1	0.070765	0.0707906	0.0707907	0.070593	0.0707
E_2	0.0810949	0.0811186	0.0811188	0.081000	0.082
$J_2(10^6)$	1115.25	1114.19	1114.19	1110.2	1080

Table 4: Application of exact solution and theory of figures to Mars.
Two-layer Mars model: $\rho_2/\rho_1 = 0.486$, $Q_V = 0.125$, $\epsilon_2 = 0.00347$.

	1st order	2nd order	3rd order	exact	observed
E_1	0.0888247	0.0888743	0.0888747	0.088859	–
E_2	0.100246	0.100294	0.100295	0.10030	0.10837
$J_2(10^6)$	1825.82	1823.18	1823.18	1823.1	1960.0

Table 5: Application of exact solution and theory of figures to Neptune. Observed values of eccentricity and gravitational coefficient are from Lindal (1992) and Jacobson (2009).

Two-layer Neptune model: $\rho_2/\rho_1 = 0.157334$, $Q_V = 0.091125$, $\epsilon_2 = 0.0254179$.

	1st order	2nd order	3rd order	exact	observed
E_1	0.143134	0.143506	0.143515	0.15147	–
E_2	0.209326	0.209642	0.209658	0.21019	0.18414
$J_2(10^6)$	6228.69	6188.61	6188.92	6241.0	3408

Table 6: Application of exact solution and theory of figures to Uranus. Observed values of eccentricity and gravitational coefficient are from Lindal (1992) and Jacobson (2007).

Two-layer Uranus model: $\rho_2/\rho_1 = 0.0883529$, $Q_{\rm V} = 0.421875$, $\epsilon_2 = 0.103112$.

	1st order	2nd order	3rd order	exact	observed
E_1	0.186917	0.187284	0.187296	0.18752	–
E_2	0.207279	0.207599	0.207616	0.20780	0.212918
$J_2(10^6)$	4847.54	4812.63	4812.62	4821.4	3341

Two-layer Uranus model: $\rho_2/\rho_1 = 0.0791231$, $Q_V = 0.0563272$, $\epsilon_2 = 0.0318902$.

	1st order	2nd order	3rd order	exact	observed
E_1	0.115322	0.115648	0.115655	0.14160	–
E_2	0.213329	0.213629	0.213648	0.21473	0.212918
$J_2(10^6)$	5718.07	5679.99	5680.32	5801.4	3341

A Level-Surface Coefficients for the Spheroidal Functions f, k and h to Order Three

The radial coordinate r, normalized to the mean radius s, can be written as follows as a truncated power series to order three in m.

$$\begin{aligned}\frac{r}{s}=&1+mf\left(\frac{1}{3}-\mu^2\right)+m^2k\left(\frac{8}{15}-4\mu^2+4\mu^4\right)+\frac{1}{18}(mf)^2\left(4-33\mu^2+27\mu^4\right)\\&+m^3h\left(\frac{26}{105}-4\mu^2+9\mu^4-5\mu^6\right)+(mf)^3\left(\frac{14}{81}-\frac{49}{18}\mu^2+5\mu^4-\frac{5}{2}\mu^6\right)\\&+(mf)\left(m^2k\right)\left(\frac{16}{63}-\frac{28}{15}\mu^2+\frac{4}{3}\mu^4\right)\end{aligned}\tag{101}$$

This expansion for r is equivalent to (32), but with the powers of m emphasized and stated explicitly. With k and h set equal to zero, it is the expansion for an ellipse with flattening mf, and with origin of coordinates at the center of the ellipse.

With this function for r/s, it is straightforward to derive the coefficients C^i_{2j} for the potential functions V_i to arbitrary order by means of (45), and by means of the procedure used to derive the coefficients C^0_{2j} in (42). For order one ($i=1$), the result for the spheroidal functions is obtained to order 2 in the form

$$\begin{aligned}C^2_0=&\frac{2}{5}f+\frac{13}{35}f^2+\frac{8}{35}k\\C^2_2=&1+\frac{4}{7}f+\frac{10}{7}f^2-\frac{16}{35}k\\C^2_4=&\frac{36}{35}f+\frac{402}{385}f^2-\frac{48}{385}k\\C^2_6=&\frac{12}{77}f^2-\frac{96}{77}k\end{aligned}\tag{102}$$

and for order two, the coefficients to first order are

$$\begin{aligned}C^4_0=&0\\C^4_2=&\frac{20}{21}f\\C^4_4=&1+\frac{200}{231}f\\C^4_6=&\frac{50}{33}f\end{aligned}\tag{103}$$

For order three, there is only one non-zero coefficient to order one, C^6_6 which is equal to one.

The coefficients for the mass contribution exterior to the level surface at β follow from (46). There is only one non-zero coefficient for order zero, the coefficient $C^{0\prime}_0$ which is equal to one. For order one the

coefficients can be written as

$$\begin{aligned}
C_0^{2\prime} &= -\frac{4}{15}f - \frac{38}{315}f^2 - \frac{16}{105}k \\
C_2^{2\prime} &= 1 - \frac{8}{21}f + \frac{32}{105}k \\
C_4^{2\prime} &= -\frac{24}{35}f - \frac{4}{55}f^2 + \frac{32}{385}k \\
C_6^{2\prime} &= \frac{32}{77}f^2 + \frac{64}{77}k
\end{aligned} \tag{104}$$

and for order 2 as,

$$\begin{aligned}
C_0^{4\prime} &= 0 \\
C_2^{4\prime} &= -\frac{16}{21}f \\
C_4^{4\prime} &= 1 - \frac{160}{231}f \\
C_6^{4\prime} &= -\frac{40}{33}f
\end{aligned} \tag{105}$$

and for order 3 there is just one non-zero coefficient $C_6^{6\prime}$ equal to one.

B Level-Surface Potential Functions

The coefficients C_{2j}^{i} and $C_{2j}^{i\prime}$ derived in Appendix A can be substituted into (51) for the potential functions. The internal normalized potential A_0 on a level surface is obtained immediately to third order as

$$\begin{aligned}
A_0 = &\left(1 + \frac{8}{45}f^2 + \frac{584}{2835}f^3 + \frac{64}{315}fk\right) S_0 + \left(\frac{2}{5}f + \frac{13}{35}f^2 + \frac{8}{35}k\right) S_2 \\
&+ S_0' - \left(\frac{4}{15}f + \frac{38}{315}f^2 + \frac{16}{105}k\right) S_2' + \left(\frac{1}{3} + \frac{4}{45}f + \frac{2}{189}f^2 + \frac{16}{315}k\right) m
\end{aligned} \tag{106}$$

Similarly, the second degree potential function A_2 is obtained immediately by (51), but it is simplified somewhat by multiplying it through by 3/2. Because it must be independent of μ on a level surface, and because it is multiplied by $P_2(\mu)$, it is equal to zero. The final expression for A_2 is

$$\begin{aligned}
A_2 = &\left(f + \frac{31}{42}f^2 + \frac{38}{63}f^3 - \frac{1}{7}h + \frac{4}{7}k + \frac{44}{105}fk\right) S_0 \\
&\left(\frac{3}{2} + \frac{6}{7}f + \frac{15}{7}f^2 - \frac{24}{35}k\right) S_2 + \frac{10}{7}fS_4 + \left(\frac{3}{2} - \frac{4}{7}f + \frac{16}{35}k\right) S_2' \\
&-\frac{8}{7}fS_4' - \left(\frac{1}{2} + \frac{10}{21}f + \frac{19}{63}f^2 + \frac{8}{15}k\right) m = 0
\end{aligned} \tag{107}$$

Because A_2 is zero, a solution for the small rotational parameter m can be found to third order. The

result is

$$\begin{aligned} m=&\left(2f-\frac{3}{7}f^2+\frac{20}{49}f^3-\frac{2}{7}h+\frac{8}{7}k-\frac{584}{245}fk\right)S_0 \\ &+\left(3-\frac{8}{7}f+\frac{524}{147}f^2-\frac{32}{7}k\right)S_2+\frac{20}{7}fS_4 \\ &+\left(3-4f+2f^2-\frac{16}{7}k\right)S_2'-\frac{16}{7}fS_4' \end{aligned} \tag{108}$$

For the higher degree potentials, the coefficients C_{2j}^{i} and $C_{2j}^{i\prime}$ are substituted into (51). Then the above expression for m is substituted into the result, and terms higher than order three are dropped. In this way the centrifugal potential enters explicitly only in A_0 and A_2. When this procedure is applied to A_4 and the result is multiplied through by 35/4, the final expression is,

$$\begin{aligned} A_4=&\left(3f^2+\frac{277}{77}f^3-\frac{48}{11}h-8k+\frac{2152}{231}fk\right)S_0 \\ &\left(15f+\frac{2385}{154}f^2+\frac{156}{11}k\right)S_2+\left(\frac{35}{4}+\frac{250}{33}f\right)S_4+16kS_2'+\left(\frac{35}{4}-\frac{200}{33}f\right)S_4'=0 \end{aligned} \tag{109}$$

Similarly for A_6, with the result multiplied through by $-33/8$, the final result is,

$$\begin{aligned} A_6=&\left(f^3-\frac{10}{7}h+\frac{32}{7}fk\right)S_0+\left(\frac{15}{14}f^2+\frac{60}{7}k\right)S_2 \\ &-\frac{25}{4}fS_4-\frac{33}{8}S_6+5fS_4'-\frac{33}{8}S_6'=0 \end{aligned} \tag{110}$$

Except for two obvious typographical errors in the m term for A_0, these expressions for A_0, A_2, A_4 and A_6 agree with expressions given by Zharkov and Trubitsyn (1978). They can of course be carried to higher order, either by introducing higher-order spheroidal functions into (32) or by extending (38) to arbitrary order, as carried out by Zharkov and Trubitsyn to fifth order (Zharkov and Trubitsyn, 1978)

C Evaluation of the Gravitational Moments

The evaluation of the gravitational moments S_{2i} and S_{2i}' that appear in the potentials A_{2i} is straightforward. An expression for r/s to arbitrary order is simply substituted into (53) and (54) and the integration is carried out over μ. The appropriate third-order expression for r/s is given by(101), and the third-order expressions for the functions ϕ_i and ϕ_i' evaluate to the following. They agree with expressions given by Zharkov and

Trubitsyn (1978).

$$
\begin{aligned}
\phi_0 &= 1 \\
\phi_2 &= -\frac{2}{5}\left(f + \frac{1}{6}f^2 + \frac{2}{9}f^3 + \frac{4}{7}k - \frac{1}{7}h + \frac{4}{3}fk\right) \\
\phi_4 &= \frac{12}{35}\left(f^2 + \frac{1}{3}f^3 + \frac{8}{9}k + \frac{16}{33}h + \frac{40}{297}fk\right) \\
\phi_6 &= -\frac{8}{21}\left(f^3 + \frac{30}{143}h + \frac{192}{143}fk\right) \\
\phi_0' &= \frac{3}{2}\left(1 - \frac{4}{45}f^2 - \frac{244}{2835}f^3 - \frac{32}{315}fk\right) \\
\phi_2' &= -\frac{2}{5}\left(f + \frac{9}{14}f^2 + \frac{8}{21}f^3 + \frac{4}{7}k - \frac{1}{7}h + \frac{4}{7}fk\right) \\
\phi_4' &= \frac{32}{105}\left(k + \frac{6}{11}h + \frac{14}{33}fk\right) \\
\phi_6' &= -\frac{80}{1001}\left(h - 4fk\right)
\end{aligned}
\tag{111}
$$

D Functions G_{ji} for the Differential Equations

As described in section 5.2, the procedure for generating the ODE of (63) sequentially produces the right-hand side of the equations as functions G_{ji} of β. The results of this process are

$$
\begin{aligned}
G_{21}=&0\\
G_{42}=&3\left(1-\frac{\delta}{S_0}\right)F_1^2+\frac{1}{2}\beta\left(2-9\frac{\delta}{S_0}\right)F_1F_1'-\frac{1}{4}\beta^2\left(1+9\frac{\delta}{S_0}\right)F_1'^2\\
G_{22}=&\frac{4}{S_0}\left(1-\frac{\delta}{S_0}\right)(F_1+\beta F_1')-5\left(1-\frac{\delta}{S_0}\right)F_1^2-2\beta\left(2-3\frac{\delta}{S_0}\right)F_1F_1'\\
&-\frac{1}{3}\beta^2\left(4-9\frac{\delta}{S_0}\right)F_1'^2-8K_2\\
G_{63}=&\frac{84}{5}\left(1-\frac{\delta}{S_0}\right)F_1^3+\frac{14}{5}\beta\left(2-9\frac{\delta}{S_0}\right)F_1^2F_1'-\frac{7}{5}\beta^2\left(1+9\frac{\delta}{S_0}\right)F_1F_1'^2\\
&+\frac{24}{5}\beta\left(4-3\frac{\delta}{S_0}\right)K_2F_1'-\frac{8}{5}\beta\left(2+9\frac{\delta}{S_0}\right)F_1K_2'+\frac{8}{5}\beta^2\left(2-9\frac{\delta}{S_0}\right)F_1'K_2'\\
&-\frac{264}{5}\frac{\delta}{S_0}F_1K_2-\frac{3}{5}\beta^3\frac{\delta}{S_0}F_1'^3\\
G_{43}=&\frac{1}{2S_0}\left(1-\frac{\delta}{S_0}\right)\left(4F_1^2+8K_2+6\beta F_1F_1'+3\beta^2F_1'^2+8\beta K_2'\right)\\
&-\frac{29}{5}\left(1-\frac{\delta}{S_0}\right)F_1^3-\frac{1}{20}\beta\left(62-159\frac{\delta}{S_0}\right)F_1^2F_1'-\frac{2}{15}\beta^2\left(2-27\frac{\delta}{S_0}\right)F_1F_1'^2\\
&+6\left(1-\frac{\delta}{S_0}\right)F_1F_2+\frac{4}{5}\left(5+31\frac{\delta}{S_0}\right)F_1K_2+\frac{1}{2}\beta\left(2-9\frac{\delta}{S_0}\right)F_1'F_2\\
&-\frac{2}{15}\beta\left(134-63\frac{\delta}{S_0}\right)F_1'K_2-\frac{2}{15}\beta^2\left(19-63\frac{\delta}{S_0}\right)F_1'K_2'-\frac{1}{2}\beta^2\left(1+9\frac{\delta}{S_0}\right)F_1'F_2'\\
&\frac{1}{2}\beta\left(2-9\frac{\delta}{S_0}\right)F_2'F_1-\frac{2}{5}\beta\left(2-21\frac{\delta}{S_0}\right)K_2'F_1-12H_3+\frac{3}{5}\beta^3\frac{\delta}{S_0}F_1'^3\\
G_{23}=&\frac{8}{3S_0^2}\left(1-\frac{\delta}{S_0}\right)(F_1+\beta F_1')\\
&-\frac{2}{3S_0}\left(1-\frac{\delta}{S_0}\right)\left(5F_1^2-6F_2+6\beta F_1F_1'+3\beta^2F_1'^2-6\beta F_2'\right)\\
&3\left(1-\frac{\delta}{S_0}\right)F_1^3+\frac{1}{5}\beta\left(18-35\frac{\delta}{S_0}\right)F_1^2F_1'-\frac{1}{15}\beta^2\left(22+45\frac{\delta}{S_0}\right)F_1F_1'^2\\
&-10\left(1-\frac{\delta}{S_0}\right)F_1F_2-\frac{8}{5}\left(5+4\frac{\delta}{S_0}\right)F_1K_2-2\beta\left(2-3\frac{\delta}{S_0}\right)F_1'F_2\\
&+\frac{16}{15}\beta\left(25-9\frac{\delta}{S_0}\right)F_1'K_2+\frac{16}{15}\beta^2\left(1-9\frac{\delta}{S_0}\right)F_1'K_2'-\frac{2}{3}\beta^2\left(4-9\frac{\delta}{S_0}\right)F_1'F_2'\\
&-2\beta\left(2-3\frac{\delta}{S_0}\right)F_2'F_1+\frac{16}{5}\beta\left(2-3\frac{\delta}{S_0}\right)K_2'F_1\\
&+12H_3-\frac{1}{45}\beta^3\left(16+33\frac{\delta}{S_0}\right)F_1'^3-8K_3
\end{aligned}
\tag{112}
$$

These general equations, when applied to a particular problem, are not as complicated as they appear. The application of Eq. 112 to the two-zone model in Sec. 5.6 illustrates the method in more detail. It illustrates

our preferred method for application of the ODE approach to any interior calculation in general.